# We are IntechOpen, the world's leading publisher of Open Access books Built by scientists, for scientists

**4,800**
Open access books available

**122,000**
International authors and editors

**135M**
Downloads

Our authors are among the

**154**
Countries delivered to

**TOP 1%**
most cited scientists

**12.2%**
Contributors from top 500 universities

CLARIVATE ANALYTICS BOOK CITATION INDEX INDEXED

WEB OF SCIENCE™

Selection of our books indexed in the Book Citation Index in Web of Science™ Core Collection (BKCI)

## Interested in publishing with us?
## Contact book.department@intechopen.com

Numbers displayed above are based on latest data collected.
For more information visit www.intechopen.com

# 4

# Predictive Modeling of Microemulsion Phase Behaviour and Microstructure Characterisation in the 1-Phase Region

Deeleep K. Rout*, Richa Goyal, Ritesh Sinha,
Arun Nagarajan and Pintu Paul
*Unilever R&D India, Whitefield, Bangalore, Karnataka*
*India*

## 1. Introduction

Microemulsions are dispersions of water and oil stabilized by one or mixtures of surfactants. The key differentiators from other dispersions are: (i) domain size of the dispersed phase is of the order of 5-100 nm in size (Schulmann et al., 1959); (ii) thermodynamically stable (Zana, 1994), and (iii) optically isotropic (Danielsson and Lindman, 1981). Commonly observed structures are: oil in water (o/w), water in oil (w/o) and bicontinuous (Scriven, 1976). Microemulsion formation has proven to be an effective approach in enhancing oil solubilisation and reducing oil-water interfacial tension (IFT) in many industrial applications. Examples include enhanced-sub surface remediation (Harwell et al., 1992; Brusseau, 1999) , drug delivery (Djordjevic et al., 2004; Kogan & Garti, 2006; Ghosh et al. , 2006), detergency (Rosen, 2004; Srivastava et al., 2006; Solans & Kuneida, 1996; Tongcumpou et al., 2006) and nano particle synthesis (Sjöblom et al., 1996). Forming an efficient microemulsion system requires an equal balance between surfactant-oil and surfactant-water interactions, which has proven to be a very challenging task for certain types of oils (e.g., vegetable oils and triglycerides) (Miller, 1991; Minana-Perez, 1996). In addition, different applications require specific degrees of solubilisation and IFT reduction. It is no surprise, then, that formulating microemulsions for specific industrial use has been referred as both an art and science (Salager, 2006). This is because microemulsion design requires not only a great understanding of molecular interactions, but also a deep understanding of thermodynamic principles (Bourel & Schechter, 1998).

Microemulsions are also known to be effective vehicles for solubilization of certain drugs and as protecting medium for the entrapped drugs from degradation, hydrolysis and oxidation. They can also provide prolonged and controlled release of the drug and prevent irritation despite the toxicity of the drug. Besides, enhanced drug penetration through the skin via microemulsion vehicles is also known (Kogan & Garti, 2006).

In order to investigate the potential of microemulsions as efficient solubilizer as well as delivery vehicles, it is necessary to characterize their microstructures as well as the locus of the

* Corresponding Author

drug or targeted molecule in the loaded microemulsion. Due to the complexity of the microemulsions and the variety of structures and components involved in the construction of the microstructure, as well as the limitation associated with each technique, the characterization of such structures is a rather difficult task. Some of the major methods relevant to the characterization of the microemulsions include viscosity (Bennett et al., 1992; Zu & Neuman, 1998; Angelico, 1998; Ray, 1994; Djordjevic, 2004; Paul, 2000; Feldman et al., 1998) , electrical conductivity measurements (Bennett et al., 1992; Zu & Neuman, 1998; Feldman et al., 1998; D'Angelo et al., 1996; Moulik et al., 2000; Feldman et al., 1996; Mukhopadhyay et al., 1996,1993; Ray et al., 1996,1993; Moulik et al., 1999; Hait et al., 2001, 2002) as well as more advanced methods such as cryo-TEM (Talmon, 1986; Regev et al., 1996; Magdassi et al., 2003), pulsed gradient spin echo (self-diffusion) NMR (Magdassi et al., 2003; Fanun et al., 2001; Spernath et al., 2003), light scattering (Kang et al., 2004; Porras et al., 2004), small angle X-Ray scattering (SAXS) (Bagger et al., 1997; Brunner-Popela et al., 1999; Yaghmur et al., 2004) and small angle neutron scattering (SANS) (Silas & Kaler, 2003; Pedersen, 2004).

Modeling the microemulsion phase transition behavior and the effect of structural parameters of compositions (surfactant structures, e.g., packing parameter, interaction parameters of surfactant mixtures, alkane number of oil ); electrolytes (type, lyotropic/hydrotropic number etc.) on phase behavior would considerably reduce experimental effort and time to obtain microemulsion systems. Although a large body of work is available in the area of predictive theoretical models of microemulsion phase behavior, predictive modeling of phase behavior dealing with real (commercial) systems/formulations is still a formidable challenge. Several theories have been proposed based on thermodynamic models (Andelman et al., 1987; Safran et al., 1986; Widom, 1996) ; Winsor-R ratio (Bourrel, M., & Schechter, 1988); packing parameter (Israelachvilli et al., 1976); hydrophilic-lipophilic balance (HLB) (Griffin, 1949); phase inversion temperature (PIT) (Shinoda & Saito, 1969); ultra-low interfacial tension (De Gennes & Taupin,1982); spontaneous curvature and bending elasticity (Hyde et al., 1997; Helfrich, 1973) and hydrophilic-lipophilic-deviation (HLD) model (Salager, 2006). Apart from thermodynamic models, as referred above, all other models are either empirical or semi-empirical models. Although, most molecular models provide an excellent qualitative predictive ability, quantitative differences exist between theory and experiment, which is attributed to a lack of exact consideration of chemical compositions in a surfactant mixture or oil mixture, mostly used for formulation developments.

Once, the condition for microemulsion is known or predicted, experimentalists and applied scientists determine its phase behavior to gain a deeper understanding of the effect of various molecular parameters (surfactant, oil and co-surfactant types and their compositions) as well as field variables (e.g., temperature, electrolyte concentration etc..) on phase changes. Different experimental methods were devised to determine phase diagrams most effectively (Kahlweit Fish diagrams) (Kahlweit, 1988) as well as Shinoda diagrams (Olsson et al., 1986). Kahlweit fish diagram is most widely used in the literature due its simplicity and useful information it provides (minimum concentration of surfactant needed to co-disperse equal amount of water and oil; minimum amount of surfactant needed to form a microemulsion; phase space to be considered for picking of a formulation). Tricritical point (i.e., an unique point in the phase space, signifying the most efficient co-dispersion of oil and water), where three distinct phases (phase separated 2-phases ($\phi$), 1-$\phi$ microemulsion and a 3-$\phi$ body co-exists) can be obtained from the fish diagram as well. As per the phase rule, there is an unique tricritical point for a

three-component system, a line of tricritical points for a four-component system and similarly, a 3-D space of tricritical points in a five component system etc..

## 2. Experimental techniques and materials

### 2.1 Electrical conductivity scans to determine the optimum salinity as well as 1-ϕ microstructure

DC electrical conductivity measurements to detect the phase inversion (from oil in water to water in oil) were carried out using a Orion (Model 150) conductivity probe immersed in a well stirred-thermally jacketed vessel at 28 °C. Stirring was facilitated using a Spinot magnetic stirrer and temperature was maintained using a water bath (Haake 3). Phase inversion composition, i.e., the electrolyte concentration (ε = salt/(salt + water)) was thus determined at various R (= oil/(water+oil) values. Electrical conductivity values of 1-ϕ microemulsions at different R values are also measured using the same set up.

AC electrical conductivity measurements were made using a Hewlett Packard 4285A Precision LCR Meter at 75 KHz to 5 MHz frequency. Electrical conductivity data obtained at 75 KHz frequency is used for microstructure characterization. The choice of 75 KHz frequency is based on the fact that this frequency is high enough to prevent space charge contributions and low enough to allow ionic effects contributing to the final conductance values. A home-made liquid cell with a cell constant of 0.73 was used. Temperatures were maintained using the Julabo F25 water circulator.

### 2.2 Determination of microemulsion phase behavior

Iso-thermal microemulsion phase diagrams (or "fish diagrams") at various R values were determined by visual inspection of samples/mixtures after equilibration. The samples were weighed into centrifuge tubes and sealed. An oil blend of Caprylic Acid and light liquid paraffin oil (LLPO) in the ratio 0.5:9.5 (wt/wt) was used. Commercial linear Lauryl alcohol ethoxylates $C_{12\text{-}15}EO_{<3>}$ and $C_{12\text{-}15}EO_{<7>}$ were taken in the ratio 1:9 (wt/wt) as its cloud point corresponded to near ambient temperature conditions of 30-33°C. The contents in the centrifuge tubes were well mixed using a Spinix vortex mixture and centrifuged in a Remi (R 24) Research Centrifugation facility at 7000 rpm for 30 minutes at a pre-determined temperature. The presence of phase types (2-$\phi$, 3-$\phi$ and 1-$\phi$) was ascertained by visual inspection. In addition, the transition between $\underline{2}\phi$ and $\overline{2}\phi$ was detected by e-conductivity measurements as and when appropriate. Shinoda diagrams are also determined by visual inspection of the liquid mixture after equilibrating the samples in a graduated Tarsons plastic tube for a few hours in a water bath.

### 2.3 NMR self-diffusion measurements

NMR measurements was performed on Bruker AV 400 spectrometer with Gradient Amplifier Board (GAB) and a 5 mm BBFO (Broad Band Fluorine Observe) probe equipped with a z-gradient coil, providing a z-gradient strength (G (Gauss)) of up to 55 $Gcm^{-1}$. The self-diffusion co-efficient of oil (1.3 ppm) and water (4.7 ppm) were determined at required temperatures (28 ± 0.5°C) by monitoring the $^1H$ signal using bipolar pulsed field gradient stimulated spin echo (BPFG-SSE) technique. Bipolar gradient pulse was used to reduce the eddy current effects (Wu et al., 1995). The pulse sequence consists of two radio frequency

pulses, a 90° and 180° pulse separated in time by tau (τ). At the time 2τ, the set up produces an echo. In order to measure the self-diffusion, magnetic field gradients are applied as two short pulses with equal duration, one between 90° and 180° pulse and the another between the 180° and the spin echo. If the molecules under study diffuse between the two field gradient pluses, the spin-echo intensity will decrease compared to when the experiment is performed without a field gradient. Experiments were carried out by varying the gradient strength and keeping the other timing parameters constant (Borkovec et al., 1996). Typically, the values used in the experiment are, Δ = 500 ms, δ = 6.2 ms and G is varied from 1.8 -18 $Gcm^{-1}$ in 32 steps. The self-diffusion co-efficient (D) is given by,

$$I = Io \exp\left(\gamma^2 G^2 \delta^2 \left(\Delta - \frac{\delta}{3}\right) D\right) \quad (1)$$

where, I is the measured signal intensity, $I_o$ is the signal intensity in the absence of field gradient pulses (G = 0), γ is the gyromagnetic ratio for the $^1H$ nucleus, δ is the gradient pulse length, Δ is the time between the two gradients in the pulse sequence (Diffusion time) and D is the self diffusion coefficient of the component.

### 2.4 Rheology and viscosity measurements

Viscosity measurements were carried out using a Carrimed $CSL^{500}$ controlled stress rheometer. An acrylic-make cone and plate geometry was used to measure viscosity as a function of shear rate/stress. The viscosity values recorded at a shear rate of 20 $S^{-1}$ are used to compare across different R values.

### 2.5 Light scattering measurements

The aggregate size of the dispersed phase as well as the correlation length between water and oil domains was measured using light scattering goniometer (Brookhaven Instrument Corporation). The laser (λ=488nm) was produced by an Argon ion laser emitter (Lexel Laser Inc), and the scattered light was detected at 30, 60, 90, 105, 120 and 150° by a photo multiplier (Brookhaven Instrument Corporation). The temperature was maintained at 28 ± 0.1 °C using a temperature controlled water bath (Grant Ltd). The samples were filtered using 0.45 micron filters into pre cleaned vials (washed with methanol) supplied by Brookhaven Instrument Corporation. The viscosity for o/w microemulsions, i.e. from R = 0 to R = 0.4, was taken as that correspond to 15 % by wt. brine (2.62 CP) solution. Similarly, for bicontinuous samples i.e. from R = 0.43 to R = 0.52, a weighted average viscosity of oil and brine was taken and for w/o microemulsion, i.e. from R = 0.6 to R = 0.9, viscosity of oil system, i.e., 19 CP, was considered for estimating correlation length of oil/water domains from light scattering experiments. The refractive index of the particles was chosen as 1.47 while the refractive index of the medium was kept as 1.33 (refractive index of water). The data were analysed by using the CONTIN algorithm.

### 2.6 Materials

Most surfactants as well as all chemicals, used in the present work, were of LR grade and were used without any further purification. Sodium linear alkyl benzene sulphonates (NaLAS) was prepared in the lab by neutralizing the corresponding acid (97 % purity) with NaOH (99.9 % pure, Sigma-Aldrich). The final concentration of the surfactant was determined by

conventional hyamine titration. The surfactant amount in the final product was found to be 82 % of the NaLAS, and the rest has been 16 % by wt. water and 2 % sodium sulphate and other organic impurities. Sodium salt of alkyl ether sulphate ($C_{12}EO_{2.5}SO_4Na$, 70 % aq. paste), was obtained from Galaxy surfactants, Mumbai, India and used as received. Imbentin OA/030 (2-ethyl ethoxylated hexanol, 99 % pure) was obtained from Kolb, Singapore. Linear Lauryl alcohol ethoxylates ($C_{12\text{-}15}\,EO_{<3>}$ and $C_{12\text{-}15}\,EO_{<7>}$, Galaxy Chemicals, India, commercial grade), were used as received, without any further purification. Extended surfactant under the trade name of Alfotera 145-4S ($C_{12}$-$C_{17}$, 4 moles propylene oxide (PO)), was purchased from Sasol, Italy. Benzalkonium chloride was obtained from Sigma-Aldrich, India.

Various hydrocarbons such as d-limonene, octane, decane, dodecane were obtained from Sigma Aldrich, India and tetradecane, hexadecane from Fluka, India. Methyl esters of fatty acids were obtained from Proctor & Gamble Chemicals, USA. Light liquid paraffin oil (LLPO, Beta Cosmetics, Silvassa, India, commercial grade) and Caprylic acid (Godrej Industries, India, 80% commercial grade) were used as received. Inorganic salts used in the study such as NaCl, KCl, fused $CaCl_2$, $MgCl_2.6H_2O$, $AlCl_3$, $FeCl_3$ were procured from Merck India and were used without any further purification. In all the experiments, deionised water (pH = 6.5) was used.

## 3. Hydrophilic lipophilic deviation (HLD) – Equivalent alkane carbon number (EACN) model

A short overview of the history of HLD is given in a paper by Queste et al., 2007. As stated there, the HLD is based on the determination of the so-called optimum formulation with flexible interfacial films. At this optimum formulation composition, the surfactant affinity to the polar and apolar pseudophases of a microemulsion is equal, meaning that the free energy change of a surfactant molecule, when transferred from oil to water and vice versa, is zero. As proposed by Salager et al., 2006, HLD is a dimensionless form of the thermodynamically derived surfactant affinity difference (SAD) equation. For systems with flexible interfacial films, this point is usually found in a tri-phasic system (oil/microemulsion/water, or the Winsor III), when the oil-water interfacial tension is at the lowest. Similarly a negative and positive value of HLD suggest the formation of Winsor Type-I and Type II microemulsions respectively. Under the conditions of this optimum formulation, the HLD value is set to zero. Any changes in the systems such as temperature; type of surfactants; oil molecular weight; salt type and its amount; type and amount of co-surfactants, will then lead to a departure from the reference state, i.e., either to a positive or negative HLD value.

For nonionic surfactants and given aqueous and oil phases, the HLD value of the system is defined from a practical approach as (Salager, 2006),

$$HLD_{ni} = b(S) - k(EACN) - \varphi(a) + \alpha_T \Delta T + \sigma \tag{2}$$

where, S = concentration of electrolyte (g/100 ml); k = characteristic parameter, depending on type of surfactant head group; EACN = equivalent alkane carbon number; $\phi$ = characteristic parameter, depending on type of co-surfactants; a = mass % of co-surfactant (usually an alcohol); $\alpha_T$ = temperature coefficient; $\Delta T = T - T_{ref}$ where T is temperature of system and $T_{ref}$ is the reference temperature (25 $^oC$) at which initially phase inversion is obtained; $\sigma$ = characteristic curvature of the surfactant, which reflects the hydrophilic/lipophilic nature of the surfactant or surfactant mixtures.

For systems, containing anionic surfactants, the corresponding expression is (Salager, 2006)

$$HLD_i = Ln\,(S) - k(EACN) - \varphi(a) - \alpha_T \Delta T + \sigma \tag{3}$$

The characteristic parameters σ and k can be determined experimentally for new and unknown surfactants by varying, e.g., the salinity and searching for the equivalent temperature shift that compensates the salinity shift. Similarly, the characteristic parameter, b (for electrolyte) and ϕ, for co-surfactants are determined experimentally.

Many a times, practical situations necessitate mixtures of anionic and nonionic surfactants to achieve a desired result, e.g., reduction of the critical micellar concentration (CMC) of a surfactant mixture (Rosen 2004; Shiloach & Blankschtein, 1998; Holland, 1983; Scamehorn, 1986), foam enhancement or reduction; Kraft temperature manipulation and skin irritancy control (Rosen 2004; Shiloach & Blankschtein, 1998; Rodriguez , 1999; Theander et al. ,2003). Attempt has been made to extend the HLD model to surfactant mixtures (Acosta & Bhakta, 2009) with the following expression,

$$HLD_{mix} = X_i . HLD_i + X_{ni} . HLD_{ni} + G_{ex}/RT \tag{4}$$

where the sub index 'i' represents the ionic surfactant and 'ni' the nonionic surfactant. The term $G_{ex}/RT$ represents the excess free energy-non-ideality normalized by RT. Conceptually, $G_{ex}$ reflects the excess free energy of transferring a mole of surfactant (in the mixture) from the oil phase to the aqueous phase. Positive value of $G_{ex}/RT$ indicate that the real mixture is more hydrophobic than the ideal mixture and vice versa.

At the optimum condition (HLD = 0), in the absence of any alcohols (for a microemulsion system with anionic surfactants) or co-surfactants (for the case with nonionic surfactant), and at the reference temperature (ΔT = 0), Equations 3 and 2 are reduced to respectively,

$$\ln S* = k\,(EACN) - \sigma \tag{5}$$

and

$$bS* = k\,(EACN) - \sigma \tag{6}$$

These two equations are incredibly simple and according to Equation (5), both 'k' and 'σ' can be experimentally determined from phase inversion experiments with a number of oils with different EACNs (experimental plot between ln S* and EACN). The slope and intercept respectively provide the above 'k' and 'σ' values. Similarly, a plot of S* and EACN also yields respective surfactant characteristics parameters (for a nonionic surfactant system). This approach has been successfully attempted by Witthayapanyanon et al., 2008 for anionic surfactants.

We have determined S* values with a number of hydrocarbons (starting with *n*-octane to *n*-hexadecane) and using an anionic surfactant, Alfoterra 145-4S ($C_{14\text{-}15}$ –$(PO)_4$ $SO_4Na$), which belongs to a class of extended surfactant because of the presence of propoxylate $(PO)_4$ group near the sulfate head group.

The calculated value of 'k' and 'σ' for Alfoterra 145-4S ($C_{14\text{-}15}$ –$(PO)_4$ $SO_4Na$) respectively are 0.099 and -0.663. It has been reported in the literature (Kiran & Acosta, 2010) that the values of 'k' and 'σ' for a similar propoxylated sulfate ($C_{12\text{-}13}$ –$(PO)_8$ $SO_4Na$) are 0.087 and -0.784

respectively. These parameters have been used to describe surfactant hydrophilicity/ hydrophobicity in a more quantitative manner, e.g., a more negative value of 'σ' suggests the surfactant to be relatively more hydrophilic, while a positive 'σ' values imply a relatively hydrophobic surfactant. In order to describe the surfactant characteristics, both the surfactant parameters 'k' as well as 'σ' needs to be considered. Thus, instead of 'σ' alone, ratio of 'σ/k' is essential to determine the relative hydrophilicity or hydrophobicity of surfactant as both the terms are relative to each other.

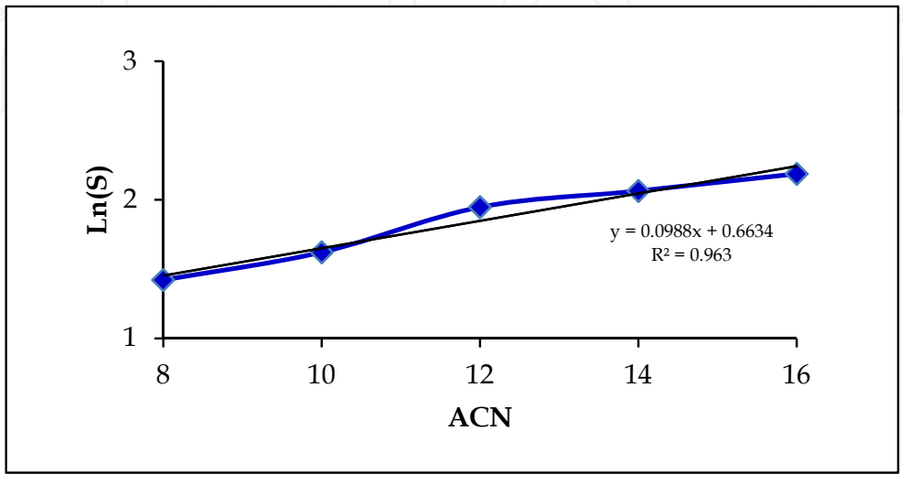


Fig. 1. Determination of k and σ using the HLD equation (4) for anionic surfactant Alfoterra 145-4S at optimal salinity at 25 °C.

Keeping the above in mind, we have obtained the ratio of σ/k for studying the effect of electrolytes on the partitioning of surfactants at the oil-water interface. Using the values of Ln(S) from Fig. 2, (σ/k) is estimated for the surfactant in presence of various electrolytes, used in the present study. Keeping the above in mind, we have tried to obtain the ratio of (σ/k) for studying the effect of electrolytes on the partitioning of surfactants at the oil-water interfaces.

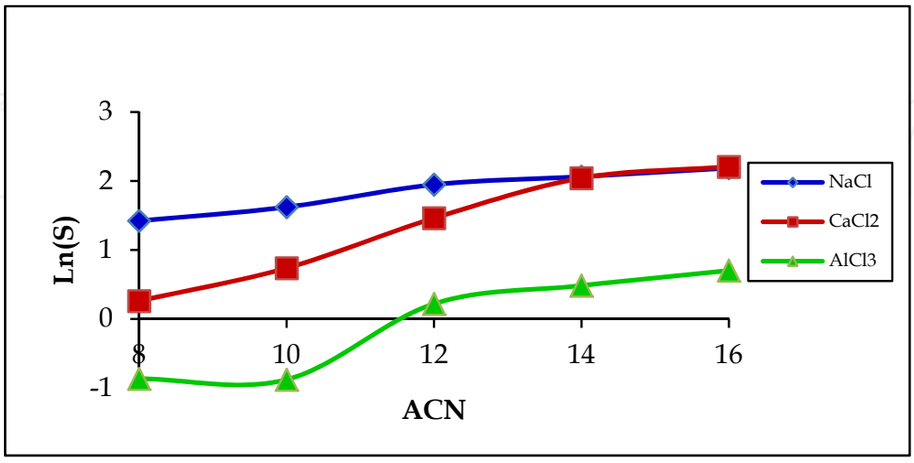


Fig. 2. Ln(S) of electrolytes with different oils (ACN) at 25 °C. The lines are drawn as a guidance to the eye.

Using the procedure outlined in the preceeding section, k, σ, and (σ/k) values are calculated for the surfactant, when various electrolytes (with multi-valent cations) are used. All the data from Fig. 2 is presented in Table 1 below.

| Salt | k | σ | $R^2$ | σ/k |
|---|---|---|---|---|
| NaCl | 0.099 | -0.66 | 0.96 | -6.71 |
| $CaCl_2$ | 0.26 | 1.78 | 0.96 | 6.83 |
| $AlCl_3$ | 0.22 | 2.77 | 0.88 | 12.30 |

Table 1. k , σ and σ/k values for Alfoterra 145-4S surfactant in the presence of various electrolytes. Oils used for this study are hydrocarbons (octane to hexadecane).

As seen in the table, $R^2$ values for $AlCl_3$ is 0.88 indicating a very poor fit to the experimental data. Surfactant hydrophobicity 'σ' is very low for mono-valent ions and it increases (from -0.6 to 2.8) as the valency of the cation increases from mono- to tri-valent ($Na^+$, $Ca^{2+}$/$Mg^{2+}$ and $Al^{3+}$) indicating an increase in the hydrophobicity of the surfactant and increasing partitioning to the oil phase. A small but finite 'σ' (~0) would indicate that the surfactant is partitioning equally well to the oil and water phases and the corresponding characteristic curvature of the oil-water interface is also close to zero. It may also be pointed out that the expression (5) is an analytic function of EACN and the intercept will always be a finite σ. The other surfactant characteristics parameter 'k', which is indicative of the surfactant head group characteristics, increases albeit slowly from a value of 0.1 (for NaCl) to 0.22 for $AlCl_3$. In a previous study by Anton et al., 2008, it was shown that 'k' remains almost constant across electrolyte types, especially when anion type is changed. It has also been commented by Salager, 1978 that 'k' values also depends on the type of electrolytes. But for most surfactants, 'k' value was found to range from 0.1 to 0.2 (Anton & Salager, 1990; Acosta& Bhakta, 2009), which is also the case in the present study. The 'k' value is a positive empirical constant determined experimentally, effectively remains the same for most head groups with the identical counterion (sodium) as seen in the past (Anton et al., 2008).

The fact that the 'k' value is changing with the valence of anions/cations, which can be attributed to the change in the head group characteristics of the surfactant due to the presence of multi-valent cations in the microemulsion. There can be two hypotheses supporting this.

The value of 'k' for sodium sulfonates is 0.1, but when a substitution of benzene or xylene moiety near the sulfonate head group takes place, it increases to 0.16. At the same time, if a $(PO)_8$ and $(EO)_2$ group is added near the head group, it decreases to 0.09 and 0.06 respectively (Witthayapanyanon et al., 2008). Benzene and xylene, being aromatic groups, will be more hydrophobic compared to propoxylene (PO) and ethoxylene (EO) groups. In addition to the surfactant head group substitution, counter-ion substitution may also affect 'k' , e.g., if sodium near the surfactant head group is replaced by calcium or aluminium, the head group characteristics may change, as reflected by a change in 'k' values.

Another argument may be made from the CMC (Critical micelle concentration) point of view, where it has been reported that in an aqueous solution of anionic Lauryl sulfates, the CMC decreases in the order, $Li^+ > Na^+ > K^+ > Cs^+ > N(CH_3)_4^+ > N(C_2H_5)_4^+ > Ca^{2+} \sim Mg^{2+}$, which is the same order as the increase in the degree of binding of the cation (i.e., $Na^+$

counterion in an aqueous medium will have the highest CMC but lower degree of binding with the head group and $Ca^{2+}$ will have lower CMC but higher degree of binding with the head group). So, an increase in the 'k' value of the surfactant, while changing counterions in solution (e.g., from $Na^{+}$ to $Ca^{2+}$ ), can be attributed to a higher degree of binding of the cation to surfactant head group. Also, the CMC value would be lower for the latter case. It is also known, for cationic surfactants, that as the degree of binding of the surfactant head group to cation increases, its area decreases (Rosen, 2004).

In the present work as well as past work (Anton et al., 2008; Acosta & Bhakta, 2009) , analysis of σ/k suggests that the value lies between -50 to +20. The lower limit is probably more or less certain as the value for sodium Lauryl ether sulfate (SLES) is -48, which has an HLB value of 40.7 (one of the highest HLB surfactant). The maximum positive value for σ/k is yet to be known as more experiments are required.

Another use of the HLD-EACN model is a practical approach to estimate the EACN value of oil mixtures, modified oils (e.g., partially polymerized oils on kitchen surfaces). We have demonstrated this with an anionic surfactant mixture (a mixture of sodium dodecyl benzene sulfonate (SDBS) and SLES). A characteristic plot of (Ln S - EACN) is determined for the surfactant mixture, which is shown in Fig. 3.

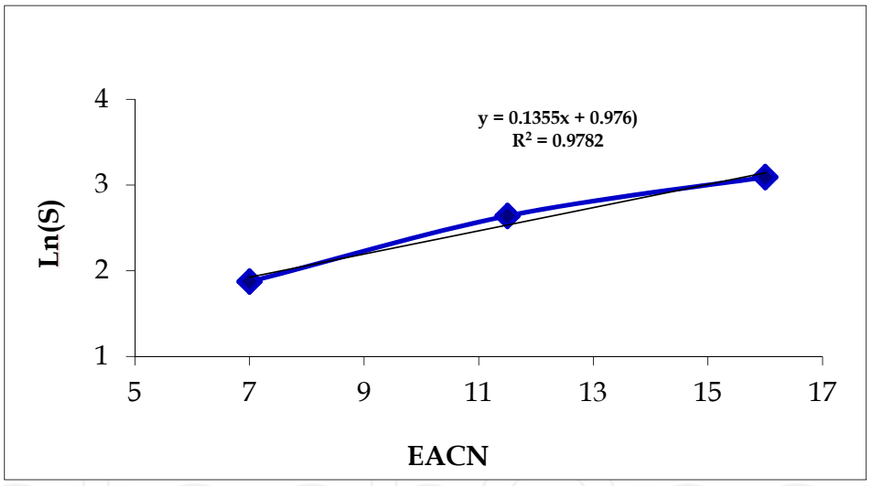


Fig. 3. Ln S- EACN plot for the surfactant mixture of sodium dodecyl benzene sulfonate and sodium Lauryl ether sulfate 1:1 by wt. NaCl is used as the salt. T = 25 °C.

The value of 'k' and 'σ' for the surfactant mixture (0.135 and -0.98 respectively) is in well agreement with reported values in the literature for anionic surfactants (Sabatini et al., 2008). Using these characteristic model parameters for the surfactant mixture, phase inversion for a 1:1 molar mixture of d-limonene (EACN = 6-7) and hexadecane (ACN = 16) is predicted to be at a S* value of 0.12, which matches well with experimentally determined value (0.14). It may be mentioned that a linear mixing rule was used to calculate the EACN value of the oil mixture from individual oil EACN/ACN values. Thus, the predictability of this model indicates that from phase inversion data (Ln S – EACN plot), one can estimate the EACN of an unknown oil by performing a phase inversion experiment with a surfactant or surfactant mixture with known characteristic 'σ/k'.

## 4. Experimental determination of microemulsion phase diagram and tricritical points

When applying microemulsions in industry or research in general, the temperature T of application, the composition of the oil, amphiphile and that of the electrolyte are specified. To describe a ternary mixture of water (A)–oil (B)–amphiphile (C), it is convenient to introduce a field variable, $X$ (e.g., temperature, co-surfactant concentration, ACN or EACN of oil, electrolyte concentration), the weight percentage of oil in the mixture of oil and water, R = (B/(A+B)), and the weight percentage of the amphiphile in the system, $\gamma$ = C/(A+B+C) (Kahlweit, 1995). Each point in the three dimensional phase space is then defined by a certain set of $X$, R and $\gamma$. In order to discuss the phase behavior, an upright phase prism is erected with $X$ as ordinate and the Gibb's ternary triangle of A-B-C as the base. The phase behavior may be discussed along either the horizontal (iso field variable) or vertical (e.g., at fixed R or $\gamma$) sections through the phase prism. For example, vertical sections of the phase prism at a fixed 'R' with the field variable $X$ along the Y-axis and $\gamma$ along the X-axis is termed the "fish diagram" (Kahlweit, 1995; Schwuger et al.,1995; Kunieda & Shinoda,1980; Kahlweit et al, 1987) (see Fig. 4). In the Fish-diagram, there is an unique coordinate, at which the 3-Φ body touches the 1-Φ region, co-existing with the 2Φ ($\underline{2}\Phi$ and $\overline{2}\Phi$), called the tri-critical point (TCP). The TCP has tremendous significance for practical applications requiring the highest mutual dispersibility between oil and water as in the case of supercritical extraction (Schwuger et al.,1995), enhanced oil recovery (Sottmann, 2002; Schwuger et al.,1995 ) and supercritical pollution oxidation (Schwuger et al.,1995).

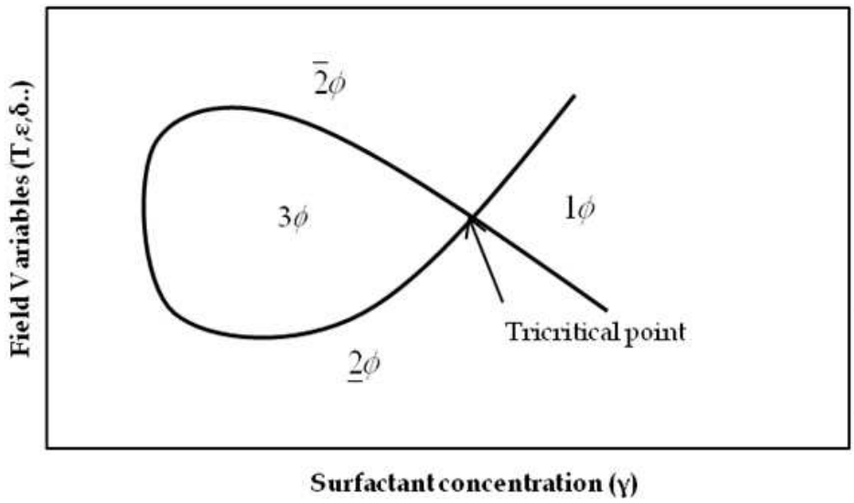


Fig. 4. Schematic representation of a Fish-diagram at a fixed R, depicting various phases and the tricritical point (TCP). The $\underline{2}\Phi$ and $\overline{2}\Phi$ respectively are identified as coexisting aqueous and oil phases with most surfactants residing in the bottom water and top oil phases respectively.

Tri-critical points vary as a function of 'R'. Kahlweit et al., 1995 have performed studies on the (*n*-decane-$C_8EO_3$-water) microemulsion system, where variations in the TCP are reported as a function of 'R', with temperature being the field variable. The trajectory of the

TCP when viewed along the temperature (T)-Gamma (γ) plane is parabolic in nature, with each tri-critical point corresponding to a given R. This trajectory shows an interesting trend, where the vertex of the parabola corresponds to the tri-critical point arising at R = 0.5. The tri-critical points corresponding to lower 'R' appear at lower temperatures than $TCP_{R=0.5}$, and tri-critical points at higher 'R' appear at higher temperatures than $TCP_{R=0.5}$, although at lower surfactant concentrations than $TCP_{R=0.5}$.

Thus, the TCP trajectory for field-variables (X) other than temperature (T), can similarly provide opportunities for applications in isothermal conditions. This provides avenues to obtain multiple compositions having ultra-low oil-water interfacial tension (IFT) at isothermal conditions, for a microemulsion that is otherwise strongly responsive to temperature (T). Further, the parabolic trajectory would be significant in predicting the variation of TCP for an unknown oil-water ratio (R). Thereby, an attempt has been made to investigate the TCP variation phenomenon for a commercial grade non-ionic surfactant based microemulsion system with electrolyte as the field variable.

### 4.1 Phase diagram (tricritical point variation) of the microemulsion system

Fig. 5. shows fish diagrams of the ternary Caprylic Acid/LLPO (0.5:9.5 wt/wt) (oil) - $C_{12\text{-}15}EO_{<3>}/C_{12\text{-}15}EO_{<7>}$ (1:9 wt/wt) (surfactant)- water system at various 'R' values. The complete fish diagram was determined only for R = 0.5, where it was found that the TCP coordinate at ε = 0.12 and γ = 0.13. At very high γ however, lamellar liquid crystalline phases are likely to appear which have not been depicted to maintain simplicity and clarity. The TCP depicting the crossover region of $\underline{2}\Phi$, $1\Phi, \bar{2}\Phi$ and $3\Phi$ corresponding to other 'R' are shown along side. Fig. 6 shows the variation of TCP with electrolyte (NaCl) concentration (ε = salt/salt+water) as the field variable.

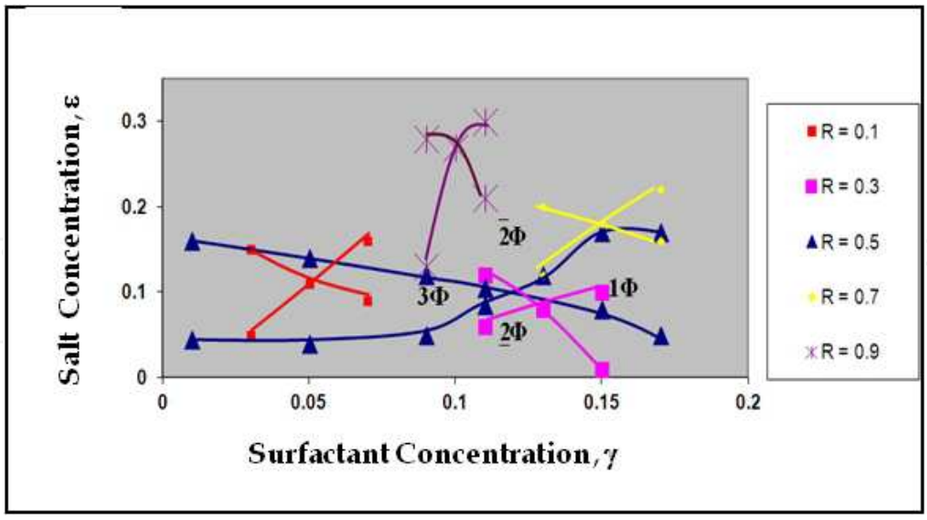


Fig. 5. Fish diagram of the ternary Caprylic Acid/LLPO (0.5:9.5 wt/wt) (oil) - $C_{12\text{-}15}EO_{<3>}/C_{12\text{-}15}EO_{<7>}$ (1:9 wt/wt) (surfactant) - water system, with epsilon denoting weight fraction of sodium chloride in water and gamma denoting the weight fraction of surfactant blend in oil and water. The complete Fish diagram is determined for R = 0.5, whereas only the TCP were determined for other R values. Temeprature = 28 °C.

The trajectory of the tri-critical points when viewed along the Epsilon (ε)-Gamma (γ) plane is again parabolic in nature, with each tri-critical point corresponding to a unique value of R. The parabola however is inclined to the X-axis and the asymmetric nature may be attributed to the commercial grade of non-ionic surfactants and oil mixtures used in the study. For $C_{12\text{-}15}$ $EO_{<3>}$ and $C_{12\text{-}15}$ $EO_{<7>}$, there exists a linear carbon chain length distribution ranging from 12-15 units for both compounds and a broad degree of ethoxylation ($EO_j$, j = 1-10), with a peak at j = 3 for $C_{12\text{-}15}EO_{<3>}$ and j = 7 for $C_{12\text{-}15}EO_{<7>}$ respectively. These also contribute to the distortions observed in the 3 Φ and 1-Φ regions [86], although the general phase behavior remains the same.

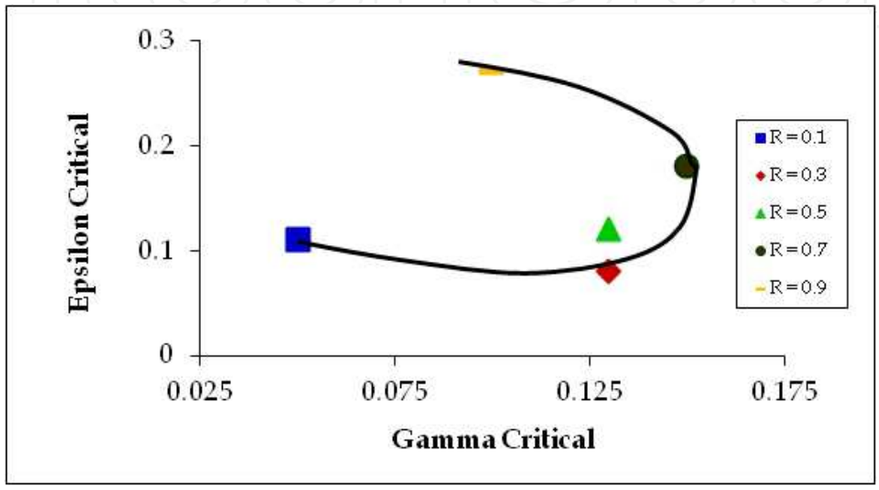


Fig. 6. Variation of TCP coordinates ($\varepsilon_{critical}$) and ($\gamma_{critical}$) as a function of oil in (oil+water) ratio R at a fixed T (= 28 °C). The line drawn though points is only for guidance.

In conclusion, tri-critical points in the present microemulsion system are seen to follow a parabolic profile as a function of R, for a field variable (electrolyte concentration, ε) similar to that observed with temperature in another ternary ($C_8E_3$-Water-Oil) system (Kahlweit et al., 1995). The similarity in the TCP variation between these two systems indicate the universality of the microemulsion phase behaviour. TCP variation as a function of electrolyte concentration also provides avenues to obtain multiple tri-critical point compositions at isothermal conditions, for a microemulsion forming system, whose phase behavior is otherwise responsive to temperature. Further, the parabolic trajectory offers a guideline to predict the location of tri-critical point compositions of a microemulsion if the oil weight fraction in the microemulsion formulation is altered. Hence, it facilitates a faster process of locating TCP compositions, where mutual dispersibility between oil and water is the maximum and oil-water interfacial tension is at the minimum.

### 4.2 Shinoda diagram of microemulsion phase behavior

Another method to study microemulsion phase behavior has been to vary the oil amount (R) in a surfactant solution with a fixed surfactant concentration (fixed γ) (also referred as Shinoda-diagram) (Sottmann et al., 2002; Olsson et al,, 2002). The field variable in this case could be one of the following: temperature; electrolyte concentration (ε); co-surfactant concentration (δ = co-surfactant/(cosurfactant + surfactant). This method is quite popular

with formulation developers as the phase diagram is determined at a low surfactant concentration. The phase diagram is shown schematically in Fig. 7.

The Shinoda- diagram or the Shinoda-cut as referred by many [86], also depicts a rich array of microstructures as seen in Fig. 7.

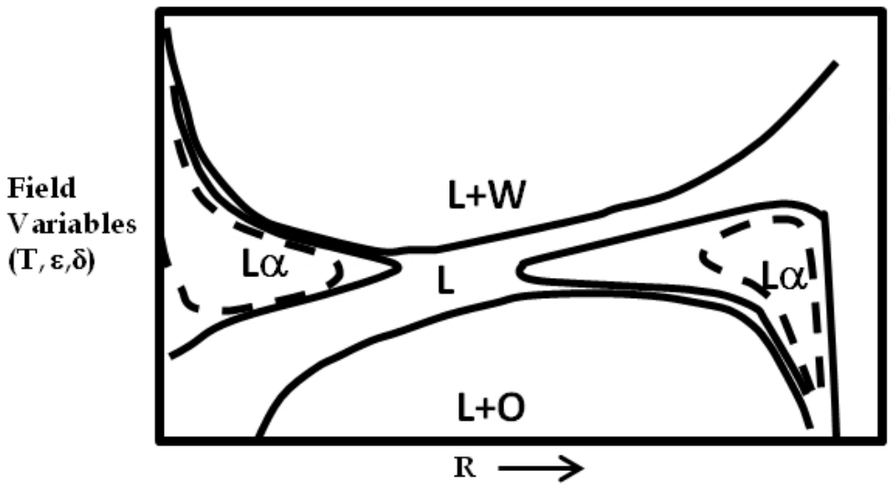


Fig. 7. A schematic Shinoda diagram, representing a rich array of phase behavior (Lamellar $L_\alpha$; 1-ϕ microemulsion, L; biphasic microemulsion and excess oil, L+O; and biphasic microemulsion and excess water, L+W), is shown at a fixed surfactant concentration (iso-γ). R is the oil to (oil+water) ratio. The phase behavior is generic (i.e., irrespective of the field variables, features of the phase diagram remain the same).

The advantage of the Shinoda diagram is that one can obtain information on the extent of oil incorporation (depicting a 1-ϕ microemulsion) at a given surfactant concentration. The above schematic diagram is a representative behavior, seen for surfactant concentrations in a range of 10-30 % by wt (γ = 0.1 to 0.3) (Sottmann et al., 2002). At lower surfactant concentrations (< γ = 0.1), the L- region will have a co-existent 1-ϕ, 3-ϕ and 2-ϕ regions, with a tri-critical point (similar to the Fish diagram) (Olsson et al,, 2002). The tricritical point in a Shinoda-diagram also indicate the maximum amount of oil, which can be dispersed in a microemulsion system (a measure of oil incorporation efficiency of a micoemulsion).

We have determined such Shinoda diagrams for a number of surfactant-oil-water systems, e.g., with benzalkonium chloride-methyl esters of *n*-alkyl fatty acid-water. Shinoda diagrams are determined with oils of increasing alkyl chain lengths (e.g., methyl ester of octanoic acid, -decanoic acid and –dodecanoic acid). Calcium chloride is used as the electrolyte. Fig. 8 shows the Shinoda diagram depicting various phases (1-ϕ; 3-ϕ and 2-ϕ regions). The 1-ϕ region is a stable, transparent liquid with an oil-in-water microstructure. The 3-ϕ region is the region, where a microemulsion phase co-exists with the excess oil and water phases. The 2-ϕ region has a microemulsion co-existing with the excess oil phase. For practical applications, the extent of 1-ϕ region is indicative of the ability of the system to provide a stable system, which can incorporate maximum oil possible. Thus, the efficiency is judged from the co-ordinate of the tri-critical point (R and ε), e.g., a higher R and lower ε is indicative of more efficient microemulsion system.

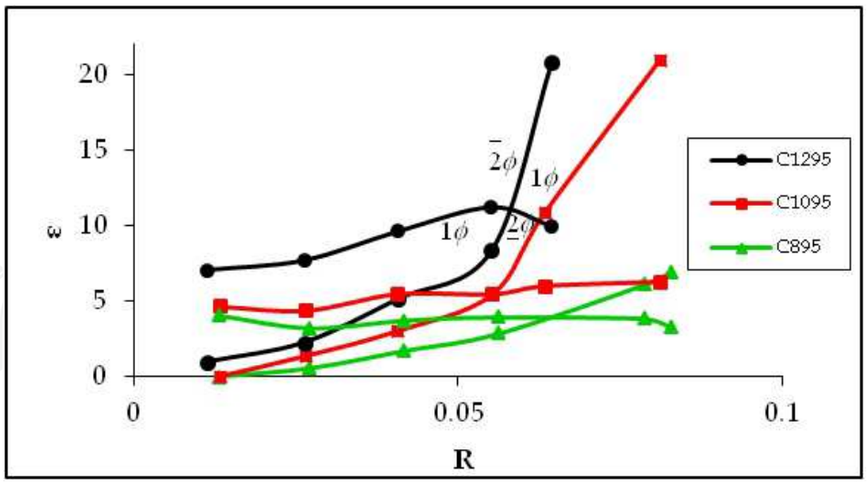


Fig. 8. Shinoda Diagram for a ternary (benzalkonium chloride-water-methyl *n*-alkanoate) with $CaCl_2$ as the electrolyte (field variable in the present case). Benzalkonium chloride concentration is 5 % by wt. ($\gamma$ = 0.05), Temperature = 25 °C.

From the Fig. 8, it is evident that a higher amount (~ 3 times) of salt is required to emulsify the higher molecular weight (MW) oil (e.g., methyl dodecanoate) compared to low MW oil (methyl octanoate). It is shown in the preceding section that there is a good correlation between electrolyte and temperature requirement for microemulsion formation as well as tri-critical point variation in the phase space. It is also well known (Kahlweit et al., 1987) that the 3-ϕ body shifts to a higher temperature, when the MW of the oil increases. In the present case, the 3-ϕ body shifts to a higher electrolyte concentration when the MW of the oil increases. On the other hand, there seems to be no difference (i.e., no major change in the R value of the tri-critical points, associated with these oils) between the two oils. In terms of microemulsion efficiency, the ratio of oil to surfactant at the tri-critical point is ~1:1, which is comparatively poor compared to some efficient microemulsion systems, known in the past with an oil to surfactant ratio at 4:1 (Shinoda et al., 1984).

## 5. Micro-structural changes in the 1-phase microemulsion region

### 5.1 Iso-electrolyte concentration phase diagram

The phase diagrams shown in Fig. 5 have presented us with an opportunity to determine the extent of single-phase domain in the ε-γ space at a fixed temperature. Thus, for a given surfactant concentration (γ= 0.2), and a given electrolyte concentration (ε = 0.15), the extent of 1-ϕ region is determined in the T-R space. As seen in Fig. 9, a wide 1-ϕ channel across R (from 0.1 to 0.9) is seen at 28 $^{o}$C with the exception for R = 0.7. Thus, it provides an opportunity to study the microstructural changes in the 1-ϕ channel using various experimental techniques. It may be mentioned here that such a 1-ϕ channel at a constant surfactant concentration ($\gamma$ = 0.2) and constant electrolyte concentration ($\varepsilon$ = 0.15) has not been reported before. Most of the past work was concerned with such channels with a varying surfactant concentration (Georges & Chen, 1986). The other advantage of the present work is also that the structural transitions can be monitored by the measurement of electrical conductivity without any unwanted contributions from varying electrolyte concentration across the 1-ϕ channel.

It may also be added here that since the current interest is to study the structural transformations across the 1-ϕ channel as a function of 'R' at a given temperature, such phase channels at other temperatures were not investigated. Subsequent measurements were limited to the 1-ϕ channel at 28 °C only.

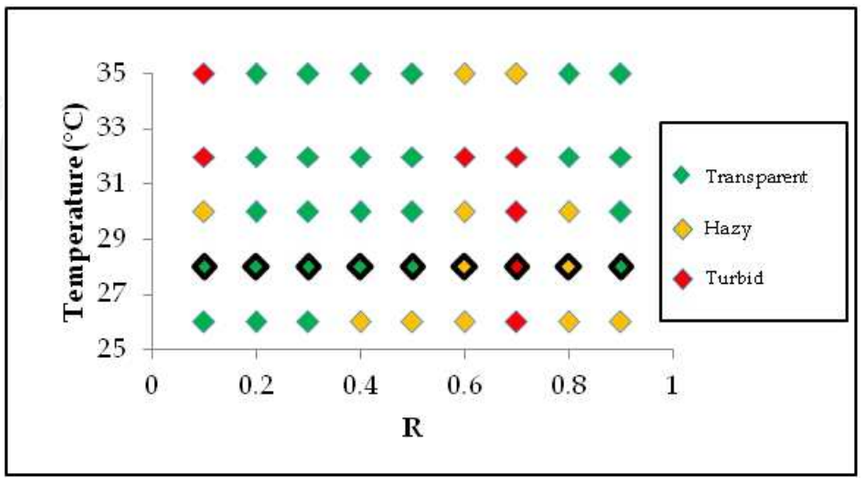


Fig. 9. 1-ϕ channel at various temperatures at a fixed surfactant concentration (γ= 0.2), and electrolyte concentration (ε = 0.15)

### 5.2 Pulsed gradient spin echo – Nuclear magnetic resonance (PGSE – NMR)

Guering and Lindman (Guering & Lindman, 1985) used the method to study molecular self-diffusion in SDS/ butanol/ toluene/ water/ NaCl microemulsion system. Garti et al (Yaghmur, 2003) and Reimer et al., 2003 used PGSE-NMR for understanding the microstructure of multi component microemulsion systems. Fanun (Fanun, 2007) has used the technique to study a non-ionic surfactant based-microemulsion system with various oils. All these above studies were carried out in the single phase region of the microemulsion. However, the concentration of all the three components was varied while scanning across the 1-ϕ channel.

The microemulsion system under study presents an opportunity to probe the microstructure variation as a function of R (oil / (oil + brine)) in the single-phase microemulsion region, but at an iso-thermal, iso-surfactant, and iso-electrolyte concentration conditions, unlike in the past. The change from oil-in-water to water-in-oil microstructure via a bicontinuous microstructure is probed by measuring the diffusion coefficient of oil and water individually in the system using self-diffusion NMR measurement. Relative self-diffusion coefficient depicted as solvent self-diffusion (D) in the microemulsion to that of the neat solvent ($D_0$) determines the domains formed by the solvent. The relative self-diffusion coefficient for water ($D^{water}/D_0^{water}$) is close to unity for an o/w microstructure while that of oil ($D^{oil}/D_0^{oil}$) is very much less than unity. High values of $D/D_0$ are observed for both oil and water in a bicontinuous structure. The self-diffusion coefficient of oil is close to $D_0^{oil}$ and that of water is very small for w/o microstructures (Sjöblom et al., 1996).

Fig. 10 shows the relative self diffusion coefficients ($D/D_0$) of oil and water in the system consisting of brine / $C_{12\text{-}15}$ $EO_{<3>}$ - $C_{12\text{-}15}$ $EO_{<7>}$ / LLPO – Caprylic acid at 28 °C as a

function of oil content (R) in the microemulsion samples where the surfactant mixture equals 20 wt % ($\gamma$ =0.2) and the salt concentration in water equals 15 wt % ($\varepsilon$ =0.15). The experimental points are joined for visual clarification. Increasing the weight fraction of oil in the 1-$\phi$ microemulsion channel $D^{oil}/D_0^{oil}$ increases from 0.14 at R=0.1 to 0.88 at R=0.8. On the other hand, the values of $D^{water}/D_0^{water}$ decrease from a value of 0.83 at R=0.1 to 0.08 at R=0.9. The relative diffusion coefficients of the oil ($D^{oil}/D_0^{oil}$) are very low for R values below 0.1 indicating droplet diffusion. These low oil diffusion values can be mainly attributed to the confinement of oils to closed domains. The gradual increase in $D^{oil}/D_0^{oil}$ values until R=0.4 suggests that percolative oil channels are beginning to form from a discrete droplet microstructure. These networked oil channels retard the water diffusion in the continuous medium resulting in a reduction in self diffusion coefficient value. At R=0.4, both values of $D^{oil}/D_0^{oil}$ and $D^{water}/D_0^{water}$ are equal, indicating a clear bicontinuous structure with solvent molecules complementing each other's mobility in their domain. It implies that the diffusion of oil or water molecules in their respective domains is not restricted by the presence of the other phase in the macroscopic distance under consideration. The increase in the $D^{oil}/D_0^{oil}$ values after R=0.4 until R=0.9 depicts a situation, where the molecular diffusion in an oil continuous channel is the dominating process. In a similar manner, the decrease in the $D^{water}/D_0^{water}$ value signifies the gradual change in confinement of water domain from continuous channel to a droplet regime. The data obtained through the NMR self-diffusion measurements is validated and supplemented with the findings from viscosity and dynamic light scattering measurements of the same system, which will be described in subsequent sections.

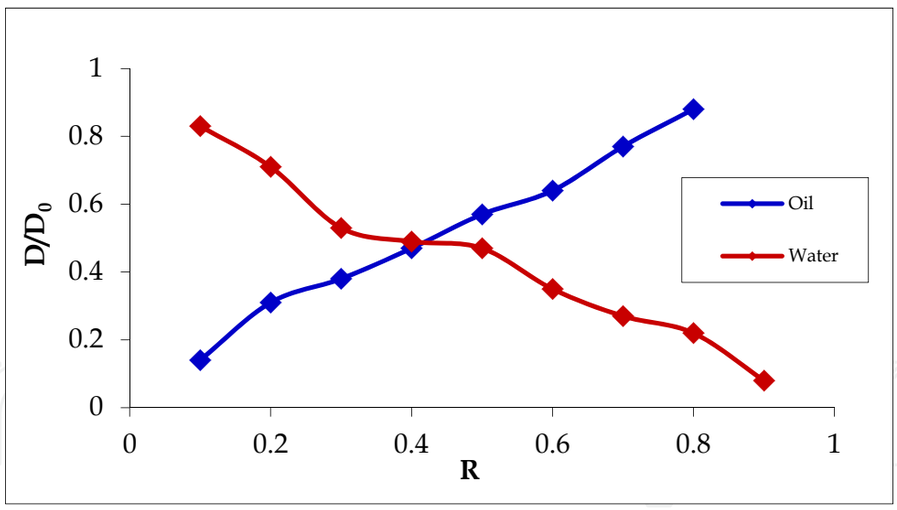


Fig. 10. Relative self diffusion coefficients ($D/D_0$) of oil and water in the single phase region of microemulsion system at iso-thermal (28 °C), iso-surfactant (20 wt. %) and iso-electrolyte concentration (15 wt. %).

### 5.3 Viscosity changes across the 1-$\phi$ channel at 28 ºC

Viscosity measurements (viscosity profile as a function of shear rate as well as viscosity measured at a given shear rate for different R) provides information on globular-bicontinuous structural transitions (Georges & Chen 1986; Georges et al., 1987; Podlogar

et al, 2004; Ajith et al., 1994; John et al., 1994). Globular (spherical oil droplets in water and vice versa) non-interacting structures are expected to exhibit a Newtonian behaviour ( $\eta \approx \dot{\gamma}^0$ ). A deviation from the Newtonian behaviour is seen when various micro-structures (either in static or under shear flow) interact with each other. Such structures are also manifested in a shear thinning behavior. Such behaviour has been reported in the past for bicontinuous structures as well (John et al. 1994). Viscosity changes as a function of shear rate have been measured at various 'R' at 28 $^{o}$C. For comparison purpose, viscosity, recorded at 20 $S^{-1}$ , are shown in Fig. 11.

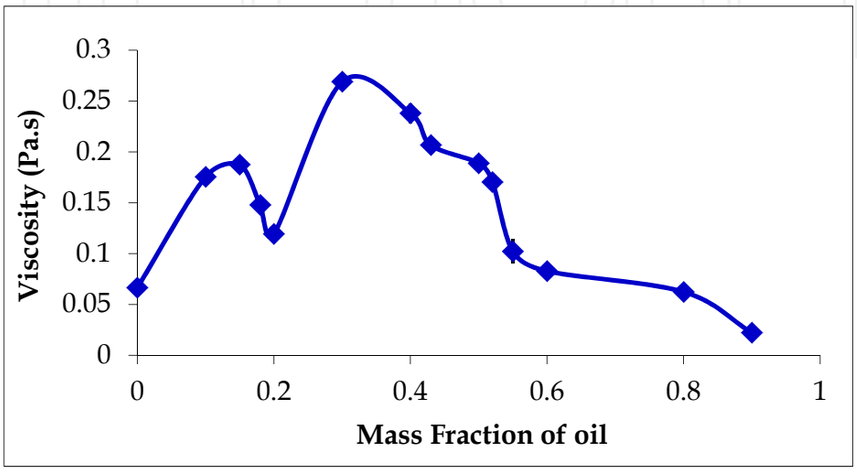


Fig. 11. Viscosity at 20 $S^{-1}$ as a function of 'R' at 28 $^{o}$C

The viscosity changes in the 1-ϕ channel is far from the bell-shaped curve as reported in the past, indicating the existence of rather more complex micro-structures with increasing oil wt. fraction. To begin with, the surfactant micellar phase (R = 0) exhibited a shear thinning behaviour as shown in Fig. 12.

It may be seen from the Fig. 12 that zero shear rate viscosity is ~1 Pa.S, which decreases to ~0.05 Pa.S at an infinite shear rate ( $\dot{\gamma}_{\infty}$ ). It is well known that nonionic surfactants form spheroidal micelles at a high surfactant concentration (Lindman, 2001) and therefore, it may be naturally expected to have such structures at $\gamma$ = 0.2. Under shear, such elongated structures either align (Larson, 1999) with each other or break down (Larson, 1999; Acharya, 2006) to spherical micelles resulting in a reduced viscosity at higher shear rates.

With increasing R, the viscosity increases till R = 0.15 (Fig. 11), following which, it decreases to 0.12 Pa.S at R = 0.18, a value slightly higher than that corresponding to R = 0 (0.08 Pa.S). Such unusual changes in the viscosity in the lower R regions may be explained as follows: With increasing oil wt. fraction, the initial elongated spheroidal micelles swell further to accommodate oil in to its hydrophobic core. Increasing in the size of the structures enhance the propensity to inter-swollen micellar interactions causing the viscosity to increase and also exhibit a stronger shear thinning behaviour ( $\eta_0 / \eta_{\infty}$ )= 50 in contrast to 20 for R = 0. This observation is also supported by the measurement of correlation length, determined via dynamic light scattering measurements (a mean diameter change from 4.8 nm to 26.2 nm) (Section 5.5). With further addition of oil, there is a rearrangement of swollen micellar structures, causing the elongated swollen, spheroidal micelles to breakdown in to smaller

spherical structures with a mean diameter of 4.7 nm. Although, the mean diameter is similar to that observed for R = 0, the structures formed at R = 0.18 are likely to be spherical, non-interacting entities, as manifested in the viscosity profiles recorded at 28 °C.

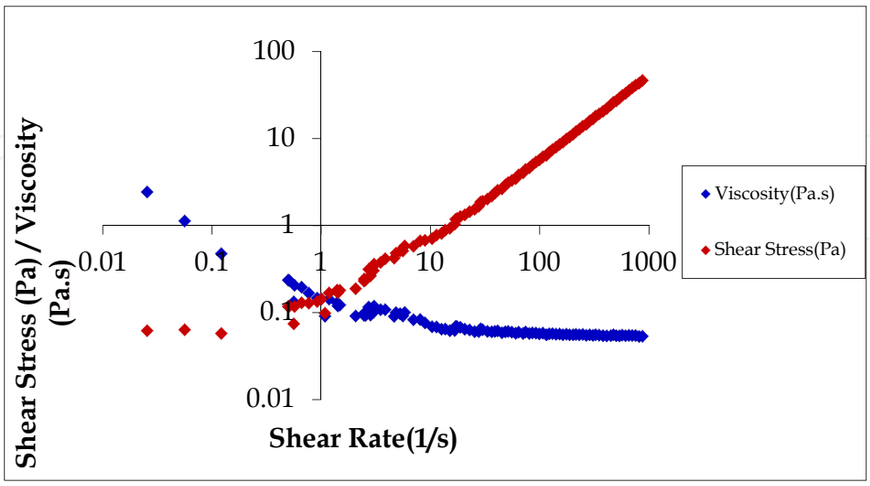


Fig. 12. Shear stress and viscosity variation as a function of shear rate at 28 °C. R = 0.

The viscosity profile for R = 0.18 indicates a Newtonian behaviour with $\eta_0 / \eta_\infty = 1$ and $\eta_0$ = 0.1 Pa.S. Subsequently with increasing R, there is a steady increase in the viscosity as seen in Fig. 11. A global maxima in viscosity (0.27 Pa.S) is seen at R = 0.3. It may be said that above R = 0.18, oil droplets exhibit a percolation behaviour, i.e., joining of globular oil droplets leading to the formation of oil channels with high $\eta_0$ values and high $\eta_0 / \eta_\infty$ values as well. For R = 0.2, these values respectively are, 10 Pa.S and 100 respectively. Thus, a transition from a Newtonian behaviour at R= 0.18 to non-Newtonian behaviour at R= 0.2 signifies the percolation threshold of oil droplets forming oil channels. The global viscosity maxima at R= 0.3 coincides with the formation of a bicontinuous microstructure, characterized by sample spanning, interpenetrating oil and water channels. In the past, both shear thinning (Saidi et al., 1990) and Newtonian flow behavior (Blom & Mellema, 1988; Peyerlasse et al., 1988; Saidi et al., 1990) was observed for bicontinuous structures at R = 0.3-0.5. However, most reports point to a Newtonian behaviour indicating that there could be occurrence of different microstructures other than bicontinuous for the R values indicated above. As observed in the past, it is expected that the bicontinuous microstructure in the 1-ϕ channel exhibits a shear thinning behaviour as well. In the present case, for R= 0.3, $\eta_0 / \eta_\infty$ is found to be ~10, which is much smaller than that observed for R = 0.2, indicating that the bicontinuous structures are much more flexible and rearrange rapidly. The mean correlation length (between oil and water channels) is found to be 10 nm, a two-fold increase from that seen at R=0.2. It is also well known (Yaghmur et al., 2003) that the correlation length approaches the maximum near the bicontinuous microstructure, before decreasing further with increasing oil wt. fr.

Following the global maxima in the viscosity at R= 0.3, it decreases subsequently with increasing R, with a shoulder near R = 0.5 (Fig. 11). Interestingly, microemulsions higher than R = 0.3 exhibit Newtonian behavior, which concurs with most past results. One possible explanation for the Newtonian behaviour for the bicontinuous microstructure is the

interfacial flexibility as well as the time scale of rearrangement of water, oil channels being much faster than the material response to external shear stimuli. The viscosity changes following the global maxima is very much similar to that seen in the past (Garti et al., 2001; Georges et al., 1987; Langevin, 1992) for 1-ϕ microemulsions with increasing oil wt. fraction. The viscosity values for microemulsions with higher R is lower than its counterpart with low R with a sharp decrease at ~ R = 0.6, which is likely to be the transition to the w/o microemulsion from a bicontinuous structure.

### 5.4 DC and AC conductivity changes in the 1-ϕ microemulsion region

The microstructural changes from a droplet morphology (e.g., w/o microemulsion) to a bicontinuous morphology via coalescence of water droplets and their percolating networks/channels have been characterized by electrical conductivity and dielectric permittivity measurements (Fanun, 2007; Yaghmur et al., 2003; Capuzzi et al., 1999; Cametti et al., 1995; Peyrelasse & Boned, 1990) . The percolation phenomena as a function of water volume fraction as well as with temperature has been studied in detail and two percolation models, i.e., static and dynamic percolation have been proposed (Cametti et al., 1995). In either of these, there is an order of magnitude change in the DC (ohmic) or low frequency electrical conductivity. The detailed nature of these curves depend on experimental design and parameters, e.g., low frequency conductivity changes at constant surfactant content, at a constant surfactant to oil ratio etc. In the present work, as mentioned earlier in the preceding sections (5.1-3), there is an opportunity to measure e-conductivity changes as a function of oil to water ratio (R) at a constant surfactant concentration (iso-γ); constant electrolyte concentration (iso-ε) and iso-thermal conditions. A plot of DC e-conductivity at various R is shown in Fig. 13.

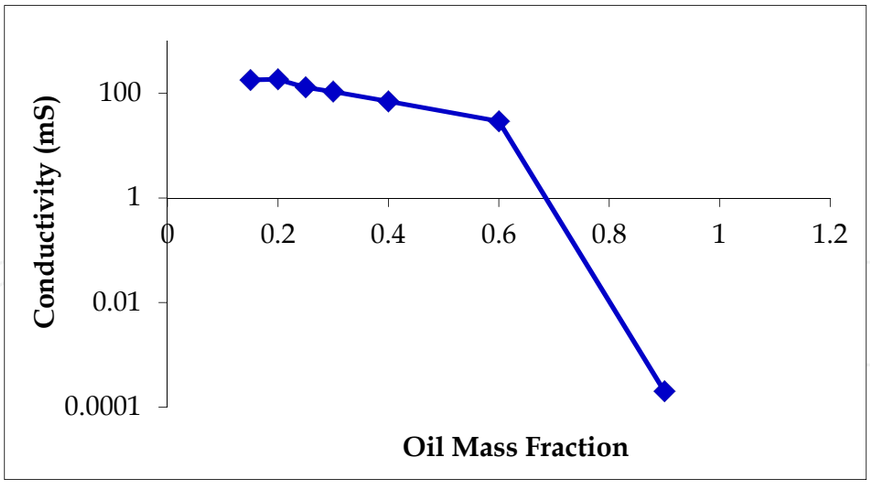


Fig. 13. DC e-conductivity changes at various R. E-conductivity could not be measured below R = 0.15 because of instrumental limitations. The line drawn across points is only for guidance to the eye.

As seen in the conductivity profile, there is a sharp drop in the conductivity values (4-5 orders of magnitude drop) after R =0.6, indicating the transition to a w/o microstructure. The above plot also shows that the percolation threshold at the water-continuous side, i.e., a

transition from o/w to bicontinuous structure occurring at R~ 0.2, manifested by a change in the slope of e-conductivity. This is expected as the conduction path is obstructed by the formation of oil channels, resulting in a decrease in the conductivity value, hence a change in the slope. On the other hand, a transition to the oil continuous from bicontinuous microstructure is signified by orders of magnitude change in the conductivity values.

AC e-conductivity scans provide a more accurate picture of electrical conductivity changes across microstructural transitions, because, at high frequency (> 10 kHz frequency), contributions from space charge polarizations can be eliminated. We measured AC conductivity at 75 KHz and the data is shown in Fig. 14.

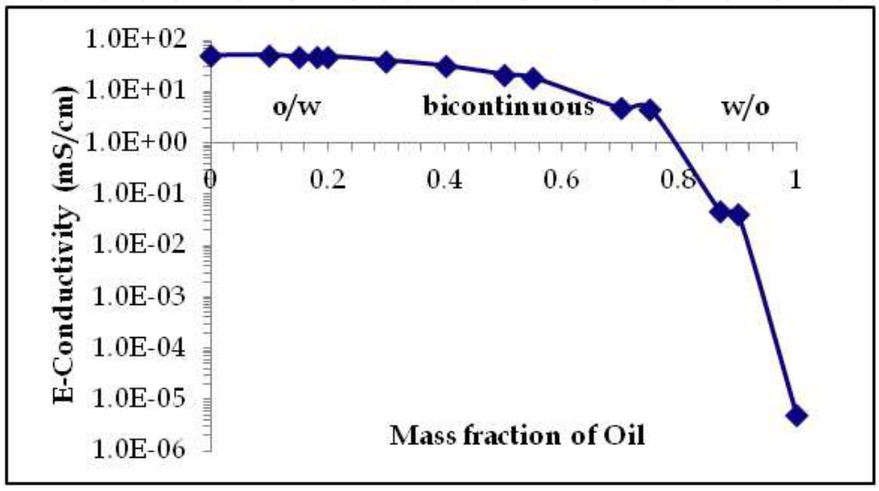


Fig. 14. AC conductivity profile in the 1-ϕ channel. The measurement is carried out at 75 KHz frequency.

The transition from the o/w microstructure to a bicontinuous one is characterized by a change in the slope of conductivity values as is the case in DC conductivity (Fig. 13). However, many a times, because of the high electrolyte concentration in the system, physical measurements become difficult in the case of DC conductivity. Based on the DC- as well as AC-conductivity measurements, the microstructural transitions in the 1-ϕ channel of the current microemulsion system, as a function (R), can be said as, o/w (0.2) bicontinuous (0.75) w/o.

### 5.5 Diffusion coefficient and correlation length of oil and water micro-domains from light scattering measurements

A plot of diffusion coefficient of various microstructural entities, causing light scattering as a function of R is shown in the Fig. 15.

The diffusion coefficient measurement has reflected various transitions, described so far in the preceding section. The diffusion coefficient peaks ~ R = 0.2, which is the percolation threshold for the oil channels to form. The highest diffusion coefficient is also indicative of lowest viscosity, encountered at R = 0.18. Similarly the transition to the oil-continuous microstructure occurs at R = 0.6, followed by a lowest diffusion coefficient measured at R = 0.5. Using these diffusion coefficient data and viscosity of the continuous phase,

correlation length at various R is estimated. The Fig. 16 shows the variation of correlation length as a function of R.

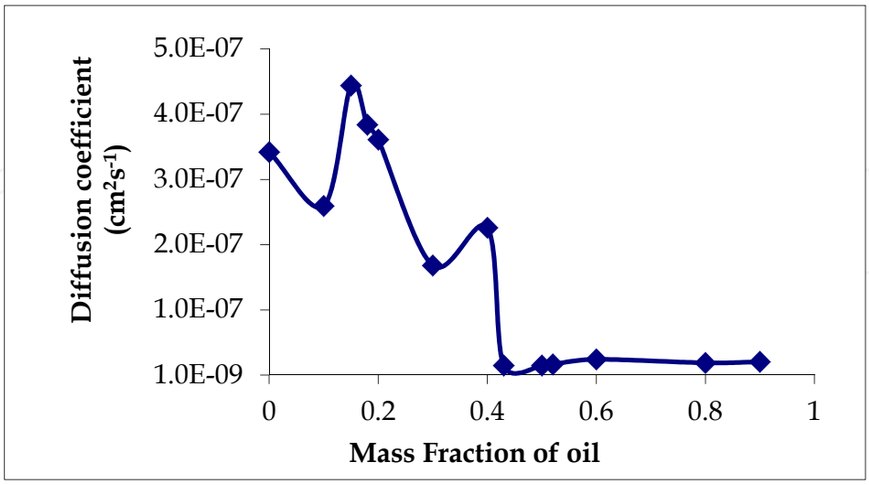


Fig. 15. Diffusion coefficient of oil/water droplets/domains in the 1-ϕ channel as determined from light scattering measurements. The line drawn though all experimental points is only a guidance to the eye.

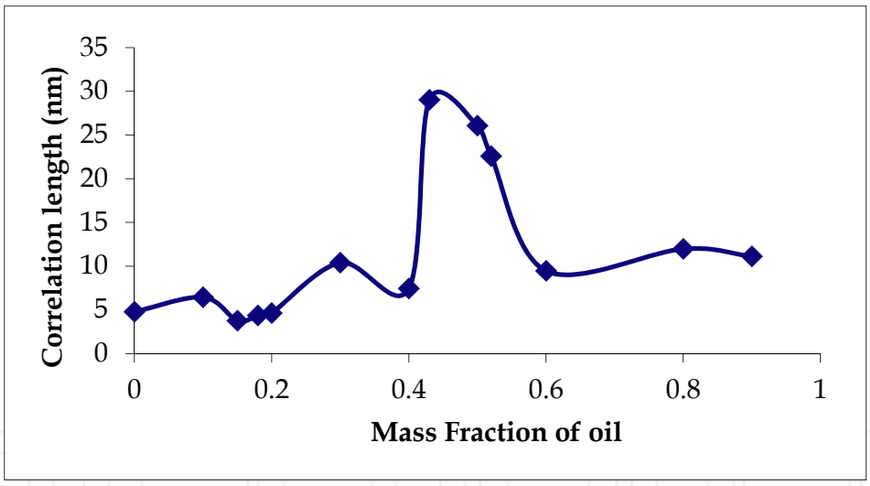


Fig. 16. Correlation length as a function of R in the 1-ϕ channel at γ = 0.2 and T = 28 °C

The correlation length changes across oil wt. fraction. Initial changes in the oil droplet size follow the changes seen in the viscosity profile (Fig. 11), i.e., an increase in the size of oil domains with increasing oil addition as well as a drop in its size at R = 0.18 (see the discussions in the preceding sections). The global maxima in the correlation length (for the bicontinuous structure) however appears at R = 0.42, which in the viscosity profile corresponds to the appearance of a shoulder. Interestingly, this is the point at which the diffusion coefficient is also the lowest and no structural breakdown of the product under shear takes place. It is common for microemulsion systems, where the correlation length passes through a maximum as per the following relation (de Gennes & Taupin, 1982; Talmon & Prager, 1978)

$$\xi = \frac{6\phi_o\phi_w}{C_s\Sigma} \tag{7}$$

Where, $\xi$, $\phi_o$, $\phi_w$, $C_s$ and $\Sigma$ are respectively, the mean correlation length of oil and water micro-domains, oil volume fraction, water volume fraction, number of surfactant molecules per unit volume and cross-sectional head group area of the surfactant at the oil-water interface. The above relation is derived with the assumption that the oil and water micro-domains form a cubic lattice (Talmon & Prager, 1978). Assuming $\Sigma$ to be 50 Å$^2$, calculated $\xi$ was found to go through a maxima (13 nm) between R = 0.3 to R = 0.45. The maximum calculated correlation length is roughly half of that estimated from experiments. The source of error could be from the accurate estimation of $\Sigma$ values as well as the assumption of a close packed cubic lattice structure. Although $\Sigma$ was taken to be 50 Å$^2$ (Klose et al., 1995), the actual value could be less, especially with a very high electrolyte concentration ($\varepsilon$= 0.15).

A comment on the variation of diffusion coefficient for various structures may be appropriate here. It is seen that diffusion coefficient varies with scattering angle as,

$$D(q) = \frac{D_0 K(q\xi)}{q^2\xi^2}$$

where K is Kawasaki function,

$$K(x) = \frac{3}{4}[x^2 + 1 + (x^3 - \frac{1}{x})\tan^{-1} x] \quad .$$

Hence, a stronger variation of D(q) with q indicate the contribution of correlation length $\xi$ variations through the 2nd order correction term [$\frac{D_0}{q^2\xi^2}$] to the $D_o$ value obtained at $\theta = 90^\circ$.

Variation in the diffusion coefficient values as a function of scattering vector ($q = \frac{4\pi n Sin(\theta/2)}{\lambda}$) is the least (independent of q) and strongest for R = 0. A strong variation of correlation length with q is also indicative of asymmetric non-spherical structures in the medium, supporting conclusions of spheroidal structures at R = 0 as well as correlation length maxima at R = 0.3.

## 6. Conclusion

We have shown that the HLD–ACN model can be successfully used to predict microemulsion phase behaviour in systems containing commercial/technical ingredients/mixtures. We also have pointed out various limitations in using the model from a microemulsion formulator point of view. New insights have been obtained by estimating the characteristic surfactant parameters 'k' and 'σ'. It has also been shown that di- and tri-valent cations cause an increase in σ/k values, indicating an increase in the surfactant hydrophobicity, possibily due to an increase in the hydrophobic volume.

Following a brief description on determination of microemulsion phase diagrams (Fish-diagram and Shinoda diagrams), we have shown the generic nature of these phase diagrams, i.e., variation of tricritical points in the phase space and also presented a rare

opportunity of 1-ϕ microemulsion channel in the phase space at constant surfactant concentration (iso-γ); constant electrolyte concentration (iso-ε) and iso-thermal conditions. Microstructural transitions, i.e., from an o/w to w/o via a bicontinuous microstructure, as manifested by various experimental parameters (self-diffusion co-efficient ; viscosity; electrical-conductivity and characteristic domain sizes) are demonstrated.

## 7. Acknowledgements

We would acknowledge our discussions with many co-workers, notably Gautam Kini and Saugata Nad, who have left Unilever now, but contributed immensely during their tenure with Unilever. Similarly, we acknowledge contributions of many students, especially Siddharth Chauhan, Ashwani Aggarwal, Akanksha Agrawal, Rupsa Banerjee, Afreen Anjum, Sneha Kankaria, Ashwini Bhatt and Anushka Pandey during their student internship program with Unilever R&D Bangalore. Finally, we also acknowledge Bangalore R&D management for the encouragement provided to us for this publication.

## 8. References

Acharya, D.P., Sato, T., Kaneko, M., Singh, Y., Kunieda, H. (2006). Effect of added poly(oxyethylene) dodecyl ether on the phase and rheological behavior of worm like micelles in aqueous SDS solution. *J. Phys. Chem., B* Vol. 110, pp. 754-760.

Acosta, E., & Bhakta, A. (2009). The HLD-NAC model for mixtures of ionic and nonionic surfactants. *Journal of Surfactants and Detergents*, Vol. 12, No. 1, pp. 7-19.

Acosta, E., & Bhakta, A. (2009). The HLD-NAC model for mixtures of ionic and nonionic surfactants. *Journal of Surfactants and Detergents*, Vol. 12, No. 1, pp. 7-19.

Ajith, S., John, A.C., & Rakshit, A.K. (1994). Physicochemical studies of microemulsions. *J.Pure Appl.Chem*. Vol. *66*,pp. 509-514

Andelman, D., Cates, M. E., Roux, D., & Safran S. A. (1987). Structure and phase equilibria of microemulsions. *Journal of Chemical Physics*, Vol. 87, No. 12, pp. 7229.

Angelico, R., Palazzo G., Colafemmina, G., Cirkel, P.A., Giustini, M & Ceglie, A. (1998). Water Diffusion and Head group Mobility in Polymer-like Reverse Micelles: Evidence of a Sphere-to-Rod-to-Sphere Transition. *J. Phys. Chem. B*, Vol. 102, No. 16, pp. 2883–2889

Anton, E., Anderez, J., Bracho, C., Vejar, F., & Salager, J. (2008). Practical surfactant mixing rules based on the attainment of microemulsion-oil-water Three-phase behavior systems. *Advances in the Polymer Science*, Vol. 218, pp. 83-113.

Anton, R., & Salager, J. (1990). Effect of the electrolyte anion on the salanity contribution to optimum formulation of anionic surfactant microemulsions. *Journal of Colloid and Interface Science*, Vol. 140, No. 1, pp. 75-81.

Bagger-J, Örgensen, H., Olsson, U., & Mortensen, K. (1997). Microstructure in a ternary microemulsion studied by small angle neutron scattering. *Langmuir*, Vol. 13, No. 6, (March 1997), pp.1413-1421.

Bennett, K.E., Hatfield, J.C., Davis, H.T., Macosko, C.W., & Scriven, L.E. (1982). In: *Microemulsions,* ID Robb, (Ed), pp. (65-84), Plenum Press, ISBN 0306408341, 9780306408342, NewYork.

Blom, C & Mellema, J. (1988). The rheological behavior of a microemulsion in the 3Φ region. *Journal of Dispersion Sciecne and Technology,* Vol. 5, No. 2, pp. 193-218

Borkovec, M., Eicke, H-F, Hammerich, H. & Das Gupta, B. (1988). Two percolation processes in Microemulsions, *J. Phys. Chem.,* Vol. 92, No. 206, pp. 211-109.

Bourel M. & Schechter, R. (1988). In: *Microemulsions and related systems: formulation, solvency, and physical properties*, Marcel Dekker, ISBN S0824779517, 9780824779511 New York

Bourrel, M., & Schechter, R. (1988). *Microemulsion and related systems*, Marcel Dekker, ISBN : 0824779517, New York.

Brunner-Popela, J., Mittelbach, R., Strey, R., Schuebert, K. V., Kaler, E. W., & Glatter, O. (1999). Small- angle scattering of interacting particles. III. $D_2O$-$C_{12}E_5$ mixtures and microemulsions with n-octane. *Journal of Chemical Physics,* Vol. 110, No. 21, pp.10623.

Cametti, C., Sciortino, F., Tartaglia, P., Rouch, J. & Chen, S. H. (1995). Complex electrical conductivity of water-in-oil microemulsions. *Phys. Rev. Lett.* Vol. 75, pp. 569-572.

Capuzzi, G., Baglioni, P., Gambi, C.M.C. & Shen, E.Y. (1999). Percolation phenomenon of calcium bis(2-ethylhexyl) sulfosuccinate water-in-oil microemulsions by conductivity and dielectric spectroscopy measurements. *Phys. Rev. E.* Vol. 60, pp. 792–798.

D'Angelo M., Fioretto D., Onori G., & Palmieri L. (1996). Dynamics of water-containing sodium bis(2-ethylhexyl)sulfosuccinate (AOT) reverse micelles: A high-frequency dielectric study. *Phys. Rev. E*, Vol.54, pp. 993

Danielsson, I. & Lindman. B. (1981). The definition of a microemulsion. *Colloids Surfaces*, Vol. 3, pp. 391–392.

De Gennes, P. G., & Taupin, C. (1982). Microemulsions and the flexibility of oil/water interfaces. *Journal of Physical chemistry*, Vol. 86, No. 13, pp. 2294-2304.

Djordjevic, L., Primorac M., Stupar M., & Krajisnik D. (2004). Characterization of caprylocaproyl macrogolglycerides based microemulsion drug delivery vehicles for an amphiphilic drug, . *Int. J. Pharm.,* Vol.271, pp. 11–19.

Feldman, Y., Kozlovich N., Nir I. and Garti N., Archipov V., & Idiyatullin Z. (1996). Mechanism of Transport of Charge Carriers in the Sodium Bis(2-ethylhexyl) Sulfosuccinate−Water−Decane Microemulsion near the Percolation Temperature Threshold. *J. Phys. Chem.*, Vol.100, No.9, pp. 3745-3748

Fanun M., J. (2007). Conductivity, viscosity, NMR and diclofenac solubilization capacity studies of mixed nonionic surfactants microemulsions. *Journal of Molecular Liquids*, Vol. 135, Issue 1-3, pp. 5-13.

Fanun, M., Wachtel, E., Antalek, B., Aserin, A., & Garti, N. (2001). A study of the microstructure of four-component sucrose ester microemulsions by SAXS and NMR. Colloids and Surfaces A- Physicochemical and Engineering Aspects, Vol. 180, No. 1-2, (May 2001), pp. 173-186.

Feldman, Y., Kozlovich N, Nir I & Garti N. (1995). Dielectric relaxation in sodium bis(2-ethylhexyl) sulfosuccinate–water–decane microemulsions near the percolation temperature threshold. *Phys Rev E*, Vol. 51, pp.478

Garti, N., Yaghmur, A., Leser, M., Clement, V., & Heribert, J.W. (2001). Improved Oil solubilisation in Oil/Water Food grade microemulsion in the presence of polyols and thanol. *J. Agric. Food Chem.,* 49, pp 2552-2562.

Georges, J., Chen J.W. & Arnaud, N. (1987). Microemulsion structure in the lenticular monophasic areas of Brine/SDS/Pentanol/dodecane or hexane systems: electrochemical and fluorescent studies. *Colloid & Polymer Sci.*, Vol. 265, pp.45-51.

Georges, J., Chen J.W. (1986). Microemulsion studies: Correlation between Viscosity, Electrical Conductivity, Electrochemical and Fluorescent Measurements. *Colloid and Polymer Science*, Vol. 264, pp. 896-907.

Ghosh, P.K., Majithiya, R.J., Umrethia ,M.L., & Murthy, R.S. (2006). Design and Development of Microemulsion Drug Delivery System of Acyclovir for Improvement of Oral Bioavailability, *AAPS Pharm. Sci. Technol.* Vol. 7, No. 3, Article 77

Griffin, W.C. (1949). Classification of surface active agents by HLB. *Journal of the society of Cosmetic chemicals*, Vol. 1, pp. 311.

Guering, P., & Lindman, B. (1985). Droplet and bicontinuous structures in microemulsion from multicomponent self-diffusion measurements. *Langmuir*, Vol. 1, No. 4, pp. 464-468.

Hait, S.K., Moulik, S.P., Rodgors, M.P., Burke, S. E., & Palepu, R. (2001). Physicochemical Studies on Microemulsions. 7. Dynamics of Percolation and Energetics of Clustering in Water/AOT/Isooctane and Water/AOT/Decane w/o Microemulsions in Presence of Hydrotopes (Sodium Salicylate, α- Naphthol, β-Naphthol, Resorcinol, Catechol, Hydroquinone, Pyrogallol and Urea) and Bile Salt(Sodium Cholate). *The Journal of Physical Chemistry B*, Vol.105, No. 29, pp.7145-7154.

Hait, S.K., Sanyal, A., & Moulik, S.P. (2002). Physicochemical studies on microemulsions. 8. The effects of aromatic methoxy hydrotropes on droplet clustering and understanding of the dynamics of conductance percolation in water/oil microemulsion systems. *The Journal of Physical Chemistry B,* Vol. 106, No. 48, pp. 12642-12650.

Harwell J. H., Sabatini D.A., & Knox,(1992). In: Transport and Remediation of sub surface contaminants, Harwell J. H., Sabatini D.A., Knox (Eds), American Chemical Society, ISBN 0841222231, 9780841222236 pp. 124, Washington DC.

Helfrich, W. (1973). Elastic properties of lipid bilayers – Theory and possible experiments. *Z. Naturforsch*, C28, pp. 693-703.

Holland, P., & Rubingh, D. (1983). Nonideal multicomponent mixed micelle model. *Journal of Physical Chemistry*, Vol. 87, No. 11, pp. 1984-1990.

Hyde, S., Blum, Z., Landh, S., Lidin, S., Ninham, B.W., Andersson, K., & Larsson, K. (1997). *The Language of Shape*, Elsevier, ISBN : 978-0-444-81538-5, Amsterdam

Israelachvilli, J.N., Mitchell, D.J., & Ninham, J. (1976). Theory of self-assembly of hydrocarbon amphiphiles into micelles and bilayers, *Journal of the chemical society – faraday transactions II*, Vol. 72, pp. 1525-1568.

John, A.C., & Rakshit, A.K. (1994). Phase Behavior and Properties of a Microemulsion in the Presence of NaCl. *Langmuir*. Vol. *10*, pp.2084-2087.

Kahlweit, M. (1988). Microemulsions. *Science*, Vol. 240, No. 4852, pp. 617-621.

Kahlweit, M. (1995). How to prepare microemulsions at prescribed temperature, oil and brine. *Journal of Physical Chemistry*, Vol. 99, No. 4, pp. 1281-1284.

Kahlweit, M., Strey, R., Haase, D., Kuneida, H., Schmeling, T., Faulhaber, E., Borkovec, M., Eicke, H.F., Busse, G., Eggers, F., Funck, T.H., Richmann, Magid, H., Söderman, L., Stilbs, O., Winkler, P., Dittrich,J. & Jahn, W. (1987). How to study Microemulsion. *J. of Colloid and Interface Science*, Vol. 118, No. 2, pp. 436-453.

Kang, B. K., Chon, S. K., Kim, S. H., Jeong, S. Y., Kim, M. S., Cho, S. H., Lee, H. B., & Khang G. (2004). Controlled release of paclitaxel from microemulsion containing PLGA and evaluation of anti-tumor activity in vitro and in vivo. International Journal of Pharmaceutics, Vol. 286, No. 1-2, pp. 147-156.

Kiran, S., & Acosta, E. (2010). Predicting the morphology and viscosity of microemulsions using HLD-NAC model. *Industrial and Engineering Chemistry Research,* Vol. 49, No. 7, pp. 3424-3432.

Klose,G, Eisenblätter,S. Galle,J., Islamov,A. & Dietrich, U. (1995). Hydration and Structural Properties of a Homologous Series of Nonionic Alkyl Oligo (ethylene oxide) Surfactants. *Langmuir.* Vol. *11,* pp. 2889-2892.

Kogan A. ,& Garti N.(2006). *Adv. Colloid Interface Sci*. Microemulsions as transdermal drug delivery vehicles, Vol. 123 pp. 369

Kogan A., & Garti N, (2006). Microemulsions as transdermal drug delivery vehicles. *Adv. In Colloid and Interf. Sci.*, Vol. 123-12, pp. 369-385

Kogan, A., Shaler, D.E., Raviv, U., Aserin, A., & Garti, N., (1982). Formation and Characterisation of ordered Bicontinuous microemulsions. *J. Phys. Chem.,* Vol. 113, No. 31, pp. 10669-10678.

Kunieda, H., & Shinoda, K. (1980). Solution behavior and hydrophile-lipophile balance temperature in the Aerosol OT-isooctane-brine system – correlation between microemulsion and ultra low interfacial tensions. *J. of Colloid and Interface Science*, Vol. 75, No. 2, pp. 601-606.

Langevin, D., 1992, Chapter 13, In: *Multiphase Microemulsion Systems in Light Scattering by Liquid Surfaces and Complementary Technique., Surfactants Science Series vol. 41* ,D. Langevin (Ed), Marcel Dekkar Inc, ISBN: 0824786076 / ISBN-13: 9780824786076 , New York

Larson R. G., (1999), Chapter 12, In: *The Structure and Rheology of Complex Fluids*. Oxford University Press. ISBN-10: 019512197X, ISBN-13: 978-0195121971,USA

Lindman, B. (2001), Vol. 1, Chapter 19,In: *Handbook of Applied Surface and Colloid Chemistry,*. K. Holmberg, D. O. Shah, & M J Schwuger (Ed), John Wiley & Sons Ltd., ISBN: 978-0-471-49083-8, New Jersey

Magdassi, S., Ben Moshe, M., Talmon, Y., & Danino, D. (2003). Microemulsions based on anionic gemini surfactant. Colloids and Surfaces A- Physicochemical and Engineering Aspects, Vol. 212, No. 1, pp. 1-7.

Mark L. B. (1999), In: *Innovative Subsurface Remediation: Field testing of Physical, Chemical and Characterization Technologies*, M.L. Brusseau (Ed), pp. (49), American Chemical society,ISBN 0841235961, 9780841235960, Washington DC.

Minana-Perez M., Graciaa A., Lachaise J., & Salager J. (1995). *J. Colloid and Interface Sci.,* Vol. 100,pp. 217

Moulik S.P., Digout LG, Aylward W.M., & Palepu R., (2000). Studies on the Interfacial Composition and Thermodynamic Properties of W/O Microemulsions. *Langmuir,* Vol. 16, pp. No. 7, pp (3101–3106)

Moulik, S. P., De, G.C., Bhowmik, B.B., & Panda, A. K. (1999). Physicochemical Studies on Microemulsions. 6. Phase Behavior, Dynamics of Percolation, and Energetics of Droplet Clustering in Water/AOT/n-Heptane System Influenced by Additives (Sodium Cholate and Sodium Salicylate). *The Journal of Physical Chemistry B*, Vol.103, No. 34, pp. 7122-7129.

Mukhopadhyay, L., Bhattacharya, P. K., & Moulik, S. P. (1990). Additive effects on the percolation of water/AOT/decane microemulsion with reference to the mechanism of conduction. *Colloids and Surfaces*, Vol. 50, pp. 295-308.

Mukhopadhyay, L., Bhattacharya, P.K., & Moulik, S.P. (1993). Effect of Butanol and Cholestrol on the Conductance of AOT Aided Water Xylene Microemulsion. *Indian Journal of Chemistry Section A- Inorganic Physical Theoretical & Analytical Chemistry,* Vol. 32, No. 6, pp. 485-490.

Olsson, U. (2002). Specialty surfactants, In: *Handbook of Applied surface and colloid chemistry*, Holmberg, K., pp. 385-405, John Wiley & Sons Ltd., ISBN : 978-0-471-49083-8,

Olsson, U., Shinoda, K., & Lindman, B. (1986). Change of the structure of microemulsions with the hydrophile lipophile balance of nonionic surfactant as revealed by NMR self-diffusion studies. *Journal of Physical chemistry*, Vol. 90, No. 17, pp. 4083-4088.

Paul. B.K., Moulik, S.P. (2000). *Proc. Ind Natl. Sci. Acad.* Vol. 66A, pp. 449

Pedersen, J.S. (1994). Analysis of small-angle scattering data from micelles and microemulsions: free- form approaches and model fitting. *Current Opinion in Colloid & Interface Science*, Vol. 4, No. 3, pp. 190-196.

Peyerlasse, J., Moha-Ouchane, M., & Boned, C., (1988). Viscosity and the phenomenon of percolation in microemulsions *Phys. Rev. A.*, Vol. 38, No. 76, pp. 228.

Peyrelasse, J. & Boned, C. (1990). Conductivity, dielectric relaxation, and viscosity of ternary microemulsions: The role of the experimental path and the point of view of percolation theory *Phys. Rev. A.* Vol. 41, pp. 938–953.

Podlogar, F., Gašperlin, M., Tomšič, M., Jamnik, A., & Rogač, M.B. (2004). Structural characterisation of water–Tween 40®/Imwitor308®–isopropyl myristate microemulsions using different experimental methods. *International Journal of Pharmaceuticals*., Vol. *276*, pp.115-128.

Porras,M., Solans, C., Gonzalez, C., Martinez, A., Guinart, A., & Gutierrez, J.M. (2004). Studies of formation of W/O nano-emulsions. Colloids and Surfaces A-Physicochemical and Engineering Aspects, Vol. 249, No. 1-3, pp. 1413-1421.

Queste,S., Salager, J.L., Strey, R. & Aubry, J.M. (2007). The EACN scale for oil classification revisted thanks to fish diagrams, J. Colloid & Interface Sci., Vol. 312, pp. 98-107.

Ray S., Bisal S. R., & Moulik S. P. (1994). Thermodynamics of Microemulsion Formation. 2. Enthalpy of Solution of Water in Binary Mixtures of Aerosol OT and Heptane and Heat Capacity of the Resulting Systems. *Langmuir*, Vol.10, No.8, pp. 2507–2510.

Ray, S., Bisal, S. R., & Moulik, S. P. (1993). Structure and dynamics of microemulsions. Part 1.—Effect of additives on percolation of conductance and energetics of clustering in water–AOT–heptane microemulsions. *Journal of Chemical Society, Faraday Transactions*, Vol. 89, No. 17, pp. 3277- 3282.

Ray, S., Paul, S., & Moulik, S. P. (1996). Physicochemical Studies on Microemulsions: V. Additive Effects on the Performance of Scaling Equations and Activation Energy for Percolation of Conductance of Water/AOT/Heptane Microemulsion. *Journal of Colloid and Interface Science*, Vol. 183, No. 1, pp. 6-12.

Regev, O., Ezrahi, S., Aserin, A., Garti, N., Wachtel, E., Kaler, E. W., Khan, A., & Talmon, Y. (1996). A study of the microstructure of a four-omponent nonionic microemulsion by cryo-TEM, NMR, SAXS and SANS. Langmuir, Vol. 12, No. 3, pp. 668-674.

Reimer, J. & Söderman, O., Sottmann, T., Kluge, K. & Strey, R. (2003). Microstructure of Alkyl Glucoside Microemulsions: Control of Curvature by Interfacial Composition. *Langmuir,* Vol. 19, No. 26, pp 10692–10702.

Rodriguez, C., & Scamehorn, J. (1999). Modification of Kraft temperature or solubility of surfactants using surfactant mixtures. *Journal of Surfactants and Detergents*, Vol. 2, No. 1, pp. 17-28.

Rosen M.J.(2004). In: *Surfactants and Interfacial Phenomena*, pp. (353), John Wiley & Sons, ISBN 0471478180, 9780471478188, New Jersey

Safran, S. A., Roux, D., Cates, M.E., & Andelman, D. (1986). Origin of Middle-Phase Microemulsions. *Physical Review Letters*, Vol. 57, No. 4, pp. 491-494.

Saidi, Z., Mathew, C., Peyrelasse, J. & Boned, C. (1990). Percolation and critical exponents for the viscosity of microemulsions. Phy. Rev. A., Vol. 42, No.2, pp. 872-876.

Salager Jean-Louis, Antón Raquel E., Sabatini David A., Harwell Jeffrey H., & Acosta Edgar J., et al. 2005. Enhancing solubilization in microemulsions—State of the art and current trends. J. Surf. Deterg., Vol. 8, No. 1, pp. 3-21.

Salager, J. (1978). PhD Dissertation, University of Texas, Austin

Salager, J., Bourrel, M., Schechter, R., & Wade, W. (1979). Mixing rules for optimum phase-behavior formulations of surfactant-oil-water systems. Society of petroleum Engineers Journal, Vol. 19, No. 5, pp. 271-278.

Scamehorn, J. F. (1986). Phenomena in mixed surfactant system. ACS Symposium series, Vol. 311, NewYork.

Schulman, J. H., Stokenius, W.& Prince, L. M. (1959). Mechanism of Formation and Structure of Micro Emulsions by Electron Microscopy. Journal of Physical Chemistry, Vol. 63,10, pp. 1677–1680.

Schwuger, M., Stickdorn, K., & Schomacker, R. (1995). Microemulsions in technical processes. *Chemical Reviews*, Vol. 95, No. 4, pp. 849-864.

Scriven L.E. (1976). Equilibrium bicontinuous structure. *Nature*, Vol. 263, pp. 123-125.

Shiloach, A., & Blankschtein, D. (1998). Predicting micellar solution properties of binary surfactant mixtures. *Langmuir*, Vol. 14, No. 7, pp. 1618-1636.

Shinoda, K., & Saito, H. (1969). The Stability of O/W type emulsions as functions of temperature and the HLB of emulsifiers: The emulsification by PIT-method. *Journal of Colloid and Interface Science*, Vol. 30, No. 2, pp. 258-263.

Shinoda, K., Kunieda, H., Arai, T., & Saijo, H. (1984). Principles of attaining very large solubilisation (microemulsion): Inclusive understaning of the solubilisation of oil and water in aqueous and hydrocarbon media. *Journal of Physical Chemistry*, Vol. 88, No. 21, pp. 5126-5129.

Silas, J. A., & Kaler, E. W. (2003). Effect of multiple scattering on SANS spectra from bicontinuous microemulsions. *Journal of Colloid and Interfacial Science*, Vol.257, No. 2, (January 2003), pp. 291-298.

Sjöblom, J. (1996). Microemulsions-phase equilibria, characterization, structures, applications and chemical reactions. *Advances in Colloid and Interface Science* Vol. 95, pp. 125.

Sjöblom, J., Lindberg, R., & Friberg, S.E. (1996). Microemulsions — phase equilibria, characterization, structures, applications and chemical reactions. *Advances in Colloid and Interface Science*, Vol. 65, pp. 125-287.

Solans C., & Kunieda H. (1996). In: *Industrial Applications of Microemulsions*, C. Solans, H. Kunieda (Eds), pp. 375, Marcel Dekker, ISBN 0824797957, 9780824797959, New York,

Sottmann, T., Lade, M., Stolz, M. & Schomacker, R. (2002). Phase behavior of non-ionic microemulsions prepared from technical-grade surfactants. *Tenside Surfactants Detergents*, Vol. 39, No. 1, pp. 20-28.

Spernath, A., Yaghmur, A., Aserin, A., Hoffmann, R. E., & Garti, N. (2003). Self-Diffusion Nuclear Magnetic Resonance, Microstructure Transitions, and Solubilization Capacity of Phytosterols and Cholesterol in Winsor IV Food-Grade Microemulsions. Journal of Agriculture and Food Chemistry, Vol. 51, No. 8, pp. 2359-2364.

Srivastava, S., Kini, G. & Rout, D. (2006). Detergency in spontaneously formed emulsions. *J. Colloid & Interface Sci.,* vol. 304, No.1, pp. 214-221.

Talmon, Y. (1986). Imaging Surfactant Dispersions by Electron-Microscopy of Vitrified Specimens. Colloids and Surfaces, Vol. 19, No. 2-3, pp. 237-248.

Talmon,Y. & Prager,S. (1978). Statistical Thermodynamics of Phase Equilibria in Microemulsions. *J.Chem.Phys.*,Vol. *69*, pp. 2984.

Theander, K., & Pugh, R. (2003). Synergism and foaming properties in mixed nonionic/fatty acid soap surfactant systems. *Journal of Colloid and Interface science*, Vol. 267, No. 1, pp. 9-17.

Tongcumpou C., Acosta E. J., Scamehorn J. F., Sabatini D. A. and Yanumet N. (2006), Enhanced triolein removal using microemulsions formulated with mixed surfactants. *J. Surf. Deterg*. Vol. 9, No.2, pp. 181-189.

Widom, B. (1996). Theoritical Modelling: An Introduction. *Physical Chemistry Chemical Physics*, Vol. 100, No. 3, pp. 242-251.

Witthayapanyanon, A., Harwell, J., & Sabitini, D. (2008). Hydrophile-lipophile deviation (HLD) method for characterizing conventional and extended surfactants. *Journal of Colloid and Interface science*, Vol. 325, No. 1, pp. 259-266.

Wu, D., Chen, A., & Johnson, C.S. (1995). An improved Diffusion Ordered Spectroscopy incorporating Bipolar Gradient Pulses. *Journal of Magnetic Resonance, Series A*, Vol. 115, pp. 260-264

Yaghmur, A., Aserin, A., Antalek, B. & Garti, N. (2003). Microstructure Considerations of New Five-Component Winsor IV Food-Grade Microemulsions Studied by Pulsed Gradient Spin-Echo NMR, Conductivity, and Viscosity. *Langmuir*, Vol. *19,* pp. 1063-1068

Yaghmur, A., Aserin, A., Antalek, B., & Garti, N. (2003). Microstructure consideration of new five component winsor IV food grade microemulsions studied by pulsed gradient spin-echo NMR, conductivity and viscosity. *Langmuir*, Vol. 19, No. 4, pp. 1063-1068.

Yaghmur, A., DeCampo, L., Aserin, A., Garti, N.& Glatter, O. (2004). Structural characterization of five-component food grade oil-in-water nonionic microemulsions. *Physical Chemistry Chemical Physics*, Vol. 6, No. 7, pp.1524-1533.

Zana R. (1994), Microemulsions. *HCR Advanced Educational Review*, Vol. 1, pp. 145- 157.

Zu Z.J., & Neuman R.D., (1995). Reversed Micellar Solution-to-Bicontinuous Microemulsion Transition in Sodium Bis (2-Ethylhexyl) Phosphate/n-Heptane/Water System. *Langmuir,* Vol. 11,No. 4, pp1081–1086.

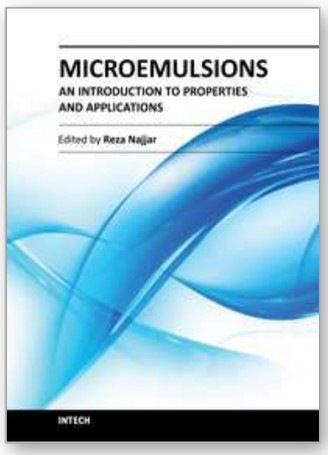


**Microemulsions - An Introduction to Properties and Applications**
Edited by Dr. Reza Najjar

ISBN 978-953-51-0247-2
Hard cover, 250 pages
**Publisher** InTech
**Published online** 16, March, 2012
**Published in print edition** March, 2012

The rapidly increasing number of applications for microemulsions has kept this relatively old topic still at the top point of research themes. This book provides an assessment of some issues influencing the characteristics and performance of the microemulsions, as well as their main types of applications. In chapter 1 a short introduction about the background, various aspects and applications of microemulsions is given. In Part 2 some experimental and modeling investigations on microstructure and phase behavior of these systems have been discussed. The last two parts of book is devoted to discussion on different types of microemulsion's applications, namely, use in drug delivery, vaccines, oil industry, preparation of nanostructured polymeric, metallic and metal oxides materials for different applications.



**InTech Europe**
University Campus STeP Ri
Slavka Krautzeka 83/A
51000 Rijeka, Croatia
Phone: +385 (51) 770 447
Fax: +385 (51) 686 166
www.intechopen.com

**InTech China**
Unit 405, Office Block, Hotel Equatorial Shanghai
No.65, Yan An Road (West), Shanghai, 200040, China
中国上海市延安西路65号上海国际贵都大饭店办公楼405单元
Phone: +86-21-62489820
Fax: +86-21-62489821

IntechOpen